EFFECTS OF SUGAR METABOLISM MUTATIONS ON ETHYLENE PRODUCTION AND RELATED TRANSCRIPT LEVELS IN DEVELOPING MAIZE SEEDS

By

ANDREW JOSEPH FUNK

A THESIS PRESENTED TO THE GRADUATE SCHOOL
OF THE UNIVERSITY OF FLORIDA IN PARTIAL FULFILLMENT
OF THE REQUIREMENTS FOR THE DEGREE OF
MASTER OF SCIENCE

UNIVERSITY OF FLORIDA

2009

To my family

ACKNOWLEDGMENTS

There are a host of people that contributed to my development, both personally and professionally, during the pursuit of this degree. I would like to acknowledge the work of my advisor, Dr. Prem Chourey, and his valuable advice throughout the process of designing, conducting, and communicating this research. Thanks to the other members of my advisory committee, Dr. Harry Klee and Dr. Wen-Yuan Song, for keeping their doors open to me even when I was too naive to ask for their help, and graciously providing assistance and critique during the final stages of my studies. Thanks to Dr. Peter Teal for believing that somewhere inside me is a worthwhile employee that just needs some direction. Thanks to Dr. Don Huber for the use of his gas chromatography equipment, and much appreciation for the expert assistance and instruction of James Lee in utilizing that equipment. Thanks to Qin Bao Li for making his wealth of experience available to me while teaching me what is important and what "doesn't matter." A special thanks to my friend and original scientific mentor, Mukesh Jain, and his wife Rani, who took me into their home and expanded my understanding of kindness and hospitality. I would like to acknowledge the good example provided by Dr. Fonsie Guilaran and his wife Lesley, whose friendship has been a source of encouragement and admonishment as I have grown into adulthood. I gladly acknowledge the unfailing love and support provided by my father Joesph, my mother Donna, and my sister Marjorie, without whom my life would be a fractured shard instead of part of a whole. Over all of these things I acknowledge God, who offers life and heals what is broken; even me.

TABLE OF CONTENTS

page

LIST OF TABLES

Table page

LIST OF FIGURES

Figure page

Abstract of Thesis Presented to the Graduate School
of the University of Florida in Partial Fulfillment of the
Requirements for the Degree of Master of Science

EFFECTS OF SUGAR METABOLISM MUTATIONS ON ETHYLENE PRODUCTION AND RELATED TRANSCRIPT LEVELS IN DEVELOPING MAIZE SEEDS

By

Andrew Joseph Funk

August 2009

Chair: Prem S. Chourey
Major: Plant Pathology

The seeds of cereal crops are critically important to the global food supply. Maize, one of the most important U.S. field crops, is an ideal model system to study cereal seed development due to its large size and well-defined tissue and cell types. Seed development is a complex process with distinct developmental phases, including cell division, cell expansion, endoreduplication, starch and protein storage, and kernel maturation. The timing and progression of kernel development is tightly regulated by factors such as sugar status and phytohormone activity. Interactions between sugars and hormones, forms of "cross-talk," have emerged as an important subject of study in recent years.

This report focused primarily on the *Mn1* gene, which encodes the INCW2 cell-wall invertase protein. The *miniature1* (*mn1*) kernel mutation eliminates INCW2 activity, which causes decreased endosperm growth and a final seed weight 30% of the wild-type value. Samples were also collected from *sugary1* (*su1*) mutant kernels deficient in a starch-debranching enzyme and a related wild-type accession as a control. Both ethylene production and related transcript levels were analyzed in these genotypes in order to compare the possible effects of genetic backgrounds and the effect of early- and late-acting metabolism mutations. Transcript

levels of three metabolic genes, *Mn1*, *Sus2* and *HXK2*, were analyzed via quantitative polymerase-chain-reaction (qPCR) techniques. Additionally, genes critical to ethylene biosynthesis and perception were included in the qPCR analysis in order to correlate transcript levels with ethylene activity. Genes under consideration were the ACC synthase genes *ACS2*, *ACS6* and *ACS7*; two ACC oxidase genes *ACO20* and *ACO35*; three ethylene receptors *ERS1-14*, *ETR2-9* and *ETR2-40*; and the DNA binding protein *EIL1-1* that is involved in downstream ethylene signaling.

Results indicated distinct bursts of ethylene in all sample series, although the quantity and timing of ethylene production varied between genetic backgrounds. The *Mn1* samples produced an increase in ethylene 13 days after pollination (DAP) that correlated with maximum published INCW2 activity. The smaller *mn1* kernels did not display a 13 DAP ethylene burst but produced 2-fold higher levels of ethylene than the wild-type between 16 and 25 DAP, coinciding with increased sucrose content in the defective endosperms. The wild-type *Su1* kernels generated two distinct peaks of ethylene production, one at 16 DAP and the second at 24 DAP. The *su1* samples did not produce the second 25 DAP burst of ethylene, despite increased sucrose levels. Results of transcript analysis indicated *HXK2* was reduced up to 2-fold in *mn1* samples during early development, consistent with the deficiency in hexoses present in that genotype. Expression of both the ACC synthase and ACC oxidase family members appeared to be related to developmental stage more than kernel genotype. The ethylene receptors displayed relatively constitutive expression, while the transcription factor *EIL1-1* was more highly expressed late in development.

CHAPTER 1
INTRODUCTION

Kernel Development

Maize seed formation is the result of coordinated development of various specialized tissues. Progress of kernel development can be monitored in terms of overlapping phases related to cell proliferation, differentiation, and maturation (Bosnes et al. 1992). Pollination results in a double-fertilization event common in angiosperms: one of the two sperm nuclei contained in a single male pollen grain fuses with an egg nuclei contained in the female megagametophyte, creating a 2N zygote. The remaining haploid sperm nucleus fuses with the two female polar nuclei, creating a 3N endosperm cell (Kiesselbach 1949; Diboll 1968). These two new cells undergo distinct but related processes, ultimately leading to a quiescent embryo ready to germinate, utilizing storage reserves contained in the terminal endosperm.

Immediately after fertilization the zygote undergoes rapid cell division to form the mass of cells that will become the embryo. The 3N endosperm cell nucleus also divides rapidly, but the absence of cytokinesis leads to a large, syncytial, highly multinucleate endosperm cell. By approximately three days after pollination (DAP) the endosperm begins cellularization, starting with the nuclei at the periphery of the cell and proceeding centripetally (Kiesselbach 1949; Kowles and Phillips 1988). Once the endosperm cells are all cellularized, they begin both cell division and expansion. From 8-12 DAP the endosperm reaches peak cell division, and after 12 DAP the cells begin the transition from differentiation to maturation, with the exception of the subaleurone region continuing division until ~20 DAP (Kiesselbach 1949; Kyle and Styles 1977). The maturation phase involves storage protein synthesis and starch loading, beginning in the central endosperm and proceeding toward the periphery ca. 15 DAP. As a part of maturation, endosperm cells undergo endoreduplication, a repetitive amplification of nuclear DNA without

normal cell division. The main onset of endoreduplication picks up as mitosis ends approximately 12 DAP, with a peak in endopolyploidy levels at 16-18 DAP (Kowles and Phillips 1985). This process is widespread in cells with high metabolic activity and is thought to facilitate the increased levels of transcription required for rapid cell enlargement and reserve storage (Grime and Mowforth 1982), although some reports have noted disparity between endoreduplication levels and cell division and enlargement (Vilhar et al. 2002). Ultimately, the purpose of endoreduplication is unclear.

Between 12 and 22 DAP, maize kernels begin accumulation of dry matter, with a coordinate increase in the presence of enzymes related to starch and storage protein biosynthesis. Expression of starch synthesis and protein synthesis genes occurs in concert with a peak at 20-25 DAP, resulting in coordinated starch synthesis in the central endosperm cells as well as oil and protein production increasing toward the aleurone and subaleurone layers (Tsai et al. 1970). The main storage carbohydrates in maize kernels are homopolymers of D-glucose: the moderately branched amylopectin, and the predominantly straight-chain amylose. The two polymers are thought to be synthesized concurrently, with the coordinated action of multiple enzymes leading to a final ratio of 3:1 amylopectin to amylose (Shannon et al. 1970; Myers et al. 2000). A third, highly-branched, water-soluble polysaccharide phytoglycogen, is detected in very small quantities but is greatly increased when various combinations of starch synthesis genes are defective (Black et al. 1966).

The first committed step in starch biosynthesis is the largely cytosolic conversion of glucose-1-phosphate (G1P) to ADP-glucose (ADP-Glc) by the enzyme ADP-glucose pyrophosphorylase (AGP) (Dickinson and Preiss 1969). AGP is a heterotetrameric enzyme encoded by the large subunit *Shrunken2* (*Sh2*) and small subunit *Brittle2* (*Bt2*) genes in maize

(Bhave et al. 1990; Preiss et al. 1990). Distinct cytosolic and plastidial forms of AGP are thought to exist, with >85% of the activity in maize endosperm coming from the cytosolic enzyme (Denyer et al. 1996; Beckles et al. 2001). ADP-glucose is transported into the amyloplast by membrane-bound BRITTLE1 (BT1) encoded by the *Bt1* gene (Shannon et al. 1998).

Inside the amyloplast, ADP-Glc monomers are linked through the formation of α-1,4 glycosidic bonds via the action of a family of at least five starch synthase (SS) enzymes. These include a granule-bound starch synthase (GBSS) encoded by the *Waxy* (*Wx*) gene and four soluble SSs designated SS1, SSIIa, SSIIb and DULL1/SSIII. Amylose is produced by GBSS1, and amylopectin is primarily the result of zSSI and DU1/SSIII activity (Shure et al. 1983; Cao et al. 1999). Two additional classes of enzymes are required to achieve the specific structure allowing amylopectin to crystallize into insoluble starch grains: starch branching enzyme (BE) and starch debranching enzyme (DBE) (Creech 1965; Nelson and Pan 1995).

Maize contains three known BEs with the ability to form branching α-1,6 glycosidic bonds via cleavage and transfer of α-1,4 bonds of linear glucose polymers (Boyer and Preiss 1978). These BEs comprise two classes in maize; BEI shows 10-fold preference for amylose (long-chain polymer) as a substrate, while BEIIa and BEIIb transfer shorter chains. It is possible that BEI provides substrate for BEIIa and BEIIb (Nelson and Pan 1995). Evidence suggests that SSs and BEs associate in multi-subunit complexes, most notably SSI/SSIIa and SSI/BEIIb (Hennen-Beirwagen et al. 2008).

The action of SSs and BEs alone results in substantial production of phytoglycogen at the expense of amylose and amylopectin (Black 1966). DBEs are required to achieve proper distribution of chain length. Two families are present in plants; isoamylases and pullulanases. The maize isoamylase is represented by *Sugary1* (*Su1*), with specificity for amylopectin but not

pullulan. The pullulanase is represented by *Zpu1*, having affinity for pullulan yet still able to attack amylopectin in a lesser fashion (Dinges et al. 2001; Wu et al. 2002). The maize *su1* mutation eliminates both isoamylase and pullulanase activity (Beatty et al. 1999).

The final stage of endosperm development is the initiation of programmed cell death (PCD). Between 16 and 20 DAP cells in the central endosperm begin to lose viability. Endonucleases dismantle DNA into fragments with sizes in multiples of 180-200 bp, first detectable at 28 DAP (Young et al. 1997). The progression of PCD follows the spatial pattern of endoreduplication and starch synthesis, initiating in the crown-proximal region and central endosperm, then proceeding down toward the base of the kernel and out toward the periphery. The only viable cells in the mature kernel are in the aleurone layer and quiescent embryo (Young and Gallie 2000a).

Ethylene Biosynthesis, Perception and Signaling

The two-carbon molecule ethylene is the simplest phytohormone identified to date, yet is involved in diverse processes related to seed germination, root and shoot elongation, senescence, fruit ripening, and both biotic and abiotic stress response (Johnson and Ecker 1998). It is a gaseous molecule able to diffuse freely through membranes, and thus the response must be tightly regulated via control of the biosynthetic and signaling machinery. Ethylene is produced in a two-step sequence beginning with ACC synthase enzymatically cleaving a structure off S-adenosyl-L-methionine to form 1-aminocyclopropane-1-carboxylic acid (ACC). The resulting ACC is rapidly converted to ethylene via the enzyme ACC oxidase. The ACC synthase step is considered rate-limiting for ethylene production (Yang and Hoffman 1984).

Ethylene is perceived via interaction with endoplasmic-reticulum (ER)-localized receptors resembling bacterial histidine and serine/threonine kinases. Five types of ethylene receptors have been identified in *Arabidopsis* to date and can be grouped into two subfamilies based on

homology (Hua and Meyerowitz 1998). Screens for *Zea mays* have yielded orthologs of two of the five receptor types established in *Arabidopsis* (Gallie and Young 2004). The two groups are ETHYLENE-RESPONSE2 (ETR2) and ETHYLENE RESPONSE SENSOR1 (ERS1). Both maize types have two members; *ZmERS1-14/ZmERS1-25* and *ZmETR2-9/ZmETR2-40*. While the gene products within the subgroups are 97% and 92% identical, respectively, the similarity between ERS1 and ETR2 is only 51% (41% identical) at the amino acid level (Gallie and Young 2004).

Ethylene receptors are negative regulators of ethylene signaling (Hua and Meyerowitz 1998). In the absence of the hormone, the receptors activate the Raf-like kinase CTR1, which is thought to control a phosphorylation cascade that ultimately represses the transcriptional regulator ETHYLENE-INSENSITIVE-3 (EIN3) (Kieber et al. 1993; Clark et al. 1998) . EIN3 and a homologous EIN3-LIKE1 (EIL1) subfamily control a transcriptional cascade related to production of diverse ethylene-responsive genes (Chao et al. 1997). EIN3 and EIL are regulated via phosphorylation state (Yoo et al. 2008) and degradation via the 26S proteasome pathway, with known F-box proteins ETHYLENE-F-BOX-1 (EBF1) and ETHYLENE-F-BOX-2 (EBF2) providing targeting specificity (Gou and Ecker 2003). ETHYLENE-INSENSIVITE-2 (EIN2) functions downstream of CTR1 to repress EBF1/2 action, while EIN2 itself is repressed by CTR1 (Alonso et al. 1999). Thus ethylene binding to the receptors inactivates CTR1, releases EIN2 from repression, hinders EBF1/2 and allows EIN3/EIL1 to initiate downstream ethylene responses.

While the majority of ethylene research has been done in *Arabidopsis* and other model systems such as tomato, some progress has been made in understanding ethylene activity in developing maize seed. Early reports quantified the pattern of ethylene production in relation to

PCD, showing two peaks of hormone accumulation in many lines tested (Young et al. 1997). It is of special importance that the patterns and absolute values of ethylene production varied between genetic backgrounds, both for wild-types and identical single-gene mutant lines. A common trend is that ethylene peaks between 12 and 16 DAP, coinciding with the first observation of cell death in the central endosperm (Young et al. 1997). A second peak of ethylene is generated roughly 28-36 DAP, accompanying the appearance of internucleosomal DNA fragmentation. In *sh2* mutant lines containing increased sucrose and glucose levels, ethylene generation is more abundant than the control: this occurs in conjunction with earlier induction of cell death as well as earlier and increased nuclease activity and a reduction in germination rate (Young et al. 1997). In addition, it has been demonstrated that PCD can be modulated by a variety of ethylene-related effects. Application of ethylene increased the severity of cell death and induction of nucleases in all lines tested, and was sufficient to cause some cell death in tissues that normally remained viable. Ethylene biosynthesis or perception inhibitors such as 2-aminoethoxyvinyl glycine (AVG) and 1-methylcyclopropene (MCP), respectively, delayed the onset and severity of PCD (Young et al. 1997; Young and Gallie 2000a). Finally, abscisic acid (ABA) has been shown to antagonize ethylene, and kernels with impaired ABA synthesis or perception generate more ethylene than controls and also show increased internucleosomal DNA fragmentation (Young and Gallie 2000b).

Gallie and Young (2004) isolated and characterized the expression of many critical components of the ethylene pathway from a collection of maize genomic and cDNA libraries. They identified three *ACS* genes, four *ACO* genes, two *ERS1*-family receptors, two *ETR2*-family receptors, a single *EIN2* and two *EIL1* members. It is of note that maize appears to lack *ETR1*, *ERS2*, and *NR* family receptors. Their attempts at isolating a *CTR* gene were unsuccessful.

Hexokinase and Sugar Signaling

The hexokinase family of enzymes catalyzes the conversion of hexose to hexose-6-phosphate in an ATP-dependent reaction. This enzyme is conserved across diverse animal, plant, and yeast species (Slein et al. 1950; Saltman 1953; Dai et al. 1995). Hexokinase is positioned at the gateway of hexose utilization as the first step in glycolysis, and has been linked to the phenomenon of hexoses as a signaling molecule in the control of diverse processes, including germination, seedling development, photosynthetic gene regulation, source/sink partitioning, flowering and senescence (Foyer 1988; Sheen 1990; Jang and Sheen 1994; Pego et al. 1999; Ohto et al. 2001). Furthermore, it was established that glucose and other hexoses, but not sugar phosphates, are the direct sugar signals causing repression of photosynthetic genes (Jang and Sheen 1994). With the discovery of distinct and separable catalytic and regulatory domains (Jang et al. 1997), hexokinases emerged as a critical component of sugar signaling. Characterization of the GLUCOSE-INSENSITIVE1 (*gin1*) mutant revealed overlap of ethylene and abscisic acid hormone pathways, with *ABA2* (*GIN1*) acting downstream of HXK1 to antagonize a branch of ethylene response related to germination, cotyledon and leaf development, and flowering (Zhou et al. 1998).

Subsequent research garnered support for the hypothesis that three sugar signaling pathways exist in higher plants: one dependent on HXK catalytic function, another related to HXK signaling, and a third functioning independent of HXKs (Xiao et al. 2000). Work by Moore et al. (2003) clearly demonstrated that HXK1-deficient *Arabidopsis* plants have altered responses to light, glucose, nitrates, and the hormones auxin and cytokinin. In addition, mutations that abolished kinase function but not glucose binding were still able to convey sugar signals, conclusively establishing the multi-functional role of hexokinases as enzymes and sugar signal transducers. *Hexokinase2* from yeast can compliment *HXK1*-deficient plants in regard to

enzymatic functions but does not restore sugar signaling in transgenic *Arabidopsis* (Moore et al. 2003). Also, AtHXK1, but not the yeast analog, associates with nuclear fractions of *Arabidopsis* cells. While only a small fraction of total HXK is found in the nucleus, there the protein interacts with two unconventional partners VHA-B1 (vacuolar H^+-ATPase B1) and RPT5B (19S regulatory particle of proteasome subunit) to directly bind DNA and regulate transcription of glucose-responsive genes (Cho et al. 2006). The key ethylene transcription factor EIN3 is specifically degraded in the presence of glucose, but this EIN3 repression is abolished in *gin2* (*hxk1*) mutants (Yanagisawa et al. 2003).

Description of Mutant Lines

The *mn1* Mutation

The primary subject of this study is the *miniature1* seed mutation, first described by Lowe and Nelson (1946). They described two groups of maize kernel mutations: the first group produced relatively normal vegetative tissues in regard to plant height, color, or vigor, yet had negative traits with respect to kernel development and nutrient quality. The second group was lethal, semi-lethal or otherwise defective during sporophytic growth. The *miniature1* locus is a member of the first group, with plants showing generally normal (albeit delayed) seedling development but producing kernels with >70% reduction in seed weight. Given the importance of maize kernels in the global food supply, seed-specific mutations involving kernel development, sugar metabolism and/or starch production are valuable tools for understanding and subsequently modifying biochemical processes for human benefit.

The *Mn1* locus encodes the INCW2 protein, an invertase enzyme anchored to the cell wall through ionic bonds (Cheng et al. 1996). Other forms of invertases are found in the cytoplasm and vacuoles, and all three types are represented in diverse plant species, catalyzing the unidirectional cleavage of sucrose into constituent glucose and fructose molecules. The *Mn1*

gene is maize endosperm-specific, with the enzyme localizing to the basal endosperm transfer cell (BETC) region that acts as a gateway for photosynthate entering the developing seed. This cell-wall invertase is thought to play a role in source-sink partitioning, acting in the apoplast to maintain a gradient for phloem unloading via sucrose cleavage, leading to hexose uptake across the BETC layer. The *mn1* gene is a naturally occurring non-lethal mutant that limits enzyme activity to less than 1% of wild-type (Miller and Chourey 1992; Chourey et al. 2006).

The earliest detectable *mn1* seed phenotype occurs at ~9-10 DAP, assessed via histological techniques showing gap formation between the pedicel and BETC layer. The phenotype is readily visualized with the naked eye as miniature seed on the cob, relative to wild-type, at the 10-12 DAP stage (Lowe and Nelson 1946; Chourey et al. 1992). In addition, *in situ* localization of both *Mn1* RNA and INCW2 protein demonstrate the absence of these molecules (Cheng et al. 1996; Li et al. 2008). These observations coincide with a significant increase in sucrose content of *mn1* seeds between 8 and 20 DAP, along with a marked decrease in glucose and fructose quantity over the same period (Li et al. 2008).

Vilhar et al. (2002) further associate the *mn1* phenotype with reduced mitotic activity and cell expansion, with no significant alteration in endoreduplication. They speculate that a high sucrose to hexose ratio during early *mn1* seed growth is a possible cause of cell differentiation and maturation at the expense of normal cell division and expansion. Recently LeClere et al. (2008) demonstrated that the auxins, indole-3-acetic acid (IAA) and IAA conjugates, are significantly reduced in *mn1* seed. Their results suggest that INCW2 directly or indirectly influences auxin biosynthesis in developing maize kernels, and this auxin deficiency could be a factor influencing reduced cell size and division in *mn1* kernels.

The *su1* Mutation

The *sugary1* locus was first identified over a century ago as a maize kernel mutation leading to a glassy, translucent mature seed (Correns 1901). Later analysis revealed an accumulation of simple sugars as well as phytoglycogen in the endosperm of homozygous *su1* kernels, corresponding to a large decrease of the predominant starch amylopectin (Creech 1965; Evensen and Boyer 1986). Beginning at 16 DAP, Creech (1965) showed that *su1* kernels maintained double the percentage of sucrose compared to wild-type. Reducing sugars were similar at 16 DAP but were 4-fold more abundant at 24 and 28 DAP in *su1* seeds. Total sugar content in *su1* seeds was double that of *Su1* kernels throughout development as a percent of dry matter, and water-soluble polysaccharides (WSPs) were increased 10-fold by 24 and 28 DAP. However, total carbohydrate was only 5-8% reduced in the *su1* genotype.

Cloning and characterization of the transcript and protein of *sugary1* led to its identification as a starch debranching enzyme (DBE) targeting the α-1,6 linkages of amylopectin and glycogen, part of the α-amylase superfamily of starch hydrolytic enzymes (James et al. 1995). The original allele *su1-Ref* contains two point mutations that lead to normal transcript levels but no protein accumulation (Dinges et al. 2001). Wild-type and *su1* transcripts are detectable as early as 8 DAP, with a slightly higher accumulation in the mutant. Enzyme levels peak toward 20 DAP in *Su1* lines but are undetectable for the duration of *su1* kernel development (Rahman et al. 1998).

CHAPTER 2
MATERIALS AND METHODS

Field Work and Fresh Material

Planting

Maize kernels from six homozygous inbred lines were planted at the University of Florida/Institute of Food and Agricultural Sciences (UF/IFAS) Plant Science Research and Education Unit (PSREU) in Citra, FL for two consecutive years. During April 2007 three different single-mutation lines, *mn1*, *sh2* and *su1* were planted. In addition to the mutant genotypes, wild-type controls were planted in equal proportion for each of the three related inbred backgrounds from which the mutants were derived. Developing ears were shoot-bagged prior to silk emergence to prevent non-specific pollination. As tassels matured and anthers began to shed pollen, tassel bags were attached to the male donor plants one day before pollen collection. Each of the six lines was self-pollinated or sibling-pollinated as material allowed. Each bag was marked with the male and female genotype used in the cross as well as the date of pollination. Once a plant was successfully pollinated, additional ears were stripped to promote growth of the target ear. After assessing the total number of ears pollinated, a harvest schedule was drawn up that would attempt to maximize sample coverage from 8 DAP through 32 DAP.

During 2008 lines were self- and sib-pollinated to maintain homozygous inbred genotypes for analysis. Pollinations were conducted between 8:30am and 10:30 am. Harvesting was done as close to 10:30 am as possible for every individual sample.

Harvest

For both years, harvesting consisted of breaking off whole ears with husk intact, sealing them in their identification bags, and depositing material in a lab refrigerator maintaining 4°C. Kernels were harvested whole onto moist paper towels for gas chromatography (GC) analysis

and then the remainder replaced in the refrigerator until they could be flash-frozen whole directly into liquid nitrogen. Any damaged kernels were discarded. Once frozen, kernels were deposited into labeled 50mL or 15mL Fisherbrand disposable conical-bottom centrifuge tubes and stored at -80°C for further analysis. Each ear was stored in a separate tube.

Gas Chromatography Analysis

The GC analysis performed in this study followed the protocol outlined by Young et al. (1997). Kernels were harvested from fresh ears and allowed to rest between moist paper towels for one hour to alleviate possible wound responses. Approximately 15 kernels were sealed in a 20mL I-CHEM borosilicate vials with 0.125 inch thick septa caps (Fischer #05-719-111), with up to three replicates per ear. Samples were allowed 3-4 hours to evolve ethylene gas. During this time a Tracor 540 GC unit feeding into a Hewlett-Packard 3396 Series III integrator was calibrated using an ethylene standard of known composition. Using a 1 mL gas-tight syringe, 0.5 mL of gas was removed from the vial head space and injected into the GC to produce a reading of parts-per-million ethylene. Data was entered into Microsoft Excel for subsequent calculations including standard error.

Nucleic Acid Preparation

RNA Isolation

Total RNA was isolated from frozen tissue using an acid-phenol lithium chloride technique adapted from Maniatis et al. (1982). A mortar and pestle were treated with chloroform, allowed to dry, and then cooled with liquid nitrogen. Two or three kernels were weighed then ground under liquid N_2 by hand, homogenized with 3 mL of isolation buffer (Table 2) and allowed to thaw. The mixture was pipetted into 14 mL round-bottom disposable polypropylene Falcon tubes (Fischer #14-959-11B), 1 mL of phenol:chloroform:isoamyl alcohol (IA) added, then mixed on a rotary shaker for 5 minutes. Samples were centrifuged at 5000 rpm for 5 minutes after which the

supernatant was mixed with 2 mL of the phenol:chloroform:IA mixture. The samples were centrifuged for 5 minutes at 5000 rpm, then the supernatant was transferred by pipette into a clean 14 mL Falcon tube along with 3 mL of chloroform:IA. The solution was mixed thoroughly and then centrifuged for 10 minutes at 5000 rpm. The aqueous phase (~2.4 mL) was then transferred to a fresh Falcon tube, mixed with an equal amount of 6M lithium chloride, and incubated at -20°C for at least one hour to precipitate RNA. The samples were then centrifuged for 30 minutes at 5000 rpm and the supernatant was discarded. The pellet was resuspended with 2 mL of 2% potassium acetate and the samples were incubated for 5 minutes at 50°C, after which 2 mL of phenol:chloroform:IA was added. The samples were mixed thoroughly and centrifuged 5 minutes at 5000 rpm. Another 2 mL of chloroform:IA was added, mixed, and centrifuged 5 additional minutes at 5000 rpm. The supernatant was carefully transferred to fresh 30 mL Corex glass tubes (DuPont Instruments #00156) containing 3 mL absolute ethanol and incubated at -20°C overnight (at least 8 hours). The samples were centrifuged at 10,000 rpm for 25 minutes, the supernatant discarded, and samples air dried. Finally the pellets were resuspended in a known volume (100-175 uL) of diethylpyrocarbonate (DEPC)-treated water, incubated at 60°C for 5 minutes, transferred to clean Eppendorf 1.5mL tubes, and quantified using a NanoDrop ND-1000 spectrophotometer (Thermo Fischer Scientific, Wilmington, DE) to calculate RNA recovered per kernel. The isolated RNA was resolved on an 0.8% agarose gel to check for quality.

DNase treatment

After initial concentration was recorded, 50 uL aliquots were taken from each sample for routine DNase treatment using the Ambion DNAfree kit (Ambion # AM1906). Five microliters of 10X DNase I buffer and one microliter rDNase I enzyme were added to each sample, mixed, and incubated at 37° for 20-30 minutes. 5.5 uL DNase Inactivation Reagent was then added and mixed by shaking and inversion several times for two minutes at room temperature. Samples

were spun down in a tabletop centrifuge for 1.5 minutes at 10,000 x g and the supernatant removed to new tubes for downstream applications. RNA quality was again verified in the same way as described in the RNA isolation protocol.

Reverse transcription

Total mRNA was converted into cDNA using the SuperScriptIII First-Strand Synthesis System (Invitrogen #18080-051). 3.5 ug DNAfree RNA was brought to a total volume of 8 uL in 200 uL PCR tubes. A master mix of dNTPs (10 mM) and Oligo$(dT)_{20}$ (50 uM) was prepared with a 1:1 ratio, and then 2 uL of the mixture was added to each 8 uL (RNA + H_2O) sample. Samples were incubated at 65°C for 5 minutes then placed on ice for at least one minute. Meanwhile a cDNA synthesis master mix was prepared consisting of, per sample: 2 uL 10X RT buffer (200 mM Tris-HCl at pH 8.4, 500 mM KCl), 4 uL 25 mM $MgCl_2$, 2 uL 0.1 M DTT, 1 uL RNase OUT™ (40 U/uL), and 1 uL SuperScript ™ III reverse-transcriptase (200 U/uL). A total of 10 uL cDNA synthesis mix was added to each sample, mixed, briefly spun in a table-top microcentrifuge, then incubated at 50ºC for 50 minutes. To stop the reaction, samples were incubated at 85ºC for 5 minutes then chilled on ice. Original RNA remaining in the reaction was digested by adding 1 uL (2 U/uL) *Escherichia coli* RNase H and incubating at 37ºC for 20 minutes. Two RT reactions were performed for each sample and used for downstream qPCR analysis.

Gene-specific Analysis

Primer Design

Primers for genes of interest were acquired by aligning gene families using Vector NTI software (Invitrogen #12605099) and searching for suitable regions of conservation or divergence, depending on desired use. For five genes related to ethylene biosynthesis, reverse primers were selected from those designed by Gallie and Young (2004). Forward primers

targeting conserved regions of homologous genes were designed using PrimerQuest software (Integrated DNA Technologies online). For *ACS2*, *ACS6*, and *ACS7*, new forward and reverse primers were designed targeting sub-300 bp amplification fragments. *Mn1*, *Hexokinase* (*HXK*) and *Sucrose-synthase2* (*Sus2*) primers were designed by Qin Bao Li in the lab. Primers for *Sugary1* (*Su1*) were adapted from James et al. (1995). See Table 2 for a complete list of primers.

Cloning

Following RT-PCR amplification of target gene fragments, PCR product was resolved on a 0.8% agarose gel stained with ethidium bromide. The Promega Benchtop 1kb DNA ladder (Fischer #PR-G7541) was used as a marker for fragment size. Once a primer pair was confirmed to produce a single band of expected size, the fragment was either purified from the remaining PCR reaction using the QIAGEN Minielute PCR Purification Kit (QIAGEN #28006) or the band was excised directly from the agarose gel and recovered using the QIAquick agarose cleanup kit (QIAGEN #28706). The purified fragment (generally 1 uL) was used in TOPO TA cloning (Invitrogen #45-0030) . The fragment was incubated at room temperature for 5 minutes in the presence of 1 uL salt solution, 1 uL TOPO2.1 PCR cloning vector, and 3 uL purified water in order to ligate the amplicon into the TOPO plasmid, forming a circular DNA structure. A vial of TOP10 OneShot chemically competent *E. coli* cells (Invitrogen #44-0301) was thawed on ice, and 2 uL of the ligation reaction was added. After 5 minutes on ice, the cells were heat-shocked at 42ºC for exactly 30 seconds to induce uptake of the recombinant DNA then placed back on ice for 1 minute to recover. In a laminar-flow hood, 250 uL of SOC medium was added to the TOP10 cells and incubated on a rotary shaker at 37ºC for 1 hour. A petri plate with solidified Luria-Bertani medium containing kanamycin was pre-warmed at 37ºC, and then the transformed TOP10 cells were spread evenly on the plate and incubated at 37°C overnight.

Single transformant *E. coli* colonies were selected and transferred to liquid LB medium containing kanamycin and incubated at 37ºC in a rotary shaker for at least 8 hours. The QIAprep Spin Miniprep Kit (QIAGEN #27106) was used to isolate plasmid DNA. The samples were transferred to 2 mL microcentrifuge tubes and spun at 10,000 rpm for 1.5 minutes to pellet cells. The supernatant was discarded, and 750 mL lysis buffer was added to each sample, vortexed at maximum speed for 30 seconds, and then allowed to rest at room temperature for 3 minutes. The solution was applied to spin columns with collection tubes and centrifuged at 14,000 rpm for 1 minute. The flow-through was discarded, and 750 mL wash buffer was applied. The samples were spun for 1 minute, flow-through discarded, and then spun one final time to remove residual wash buffer still in the spin column. The columns were transferred to fresh 1.5 mL collection tubes, 50 uL of elution buffer added to the filters, then collected by centrifugation for 1 minute at 14,000 rpm.

To verify the presence of inserts, 10 uL of plasmid eluate from each sample was digested using 1 uL EcoR1, 2 uL ReAct3 buffer and 7 uL water. The reaction was incubated at 37ºC for 1 hour then visualized on a 0.8% agarose gel as previously described.

DNA Sequencing Reaction

Plasmids containing correctly-sized inserts were sequenced using M13 primers included in the TOPO TA cloning kit (see Table 2 for primer sequence). Inserts were sequenced using the Applied Biosystems BigDye Terminator v1.1 Cycle Sequencing Kit (Fischer #NC9008533) as follows: 2uL TOPO forward primer, 2uL plasmid, 2uL BigDye and 4uL water were mixed and briefly centrifuged. The sequencing reaction consisted of 3 minutes at 95ºC, followed by 25 cycles of 95ºC for 25 seconds, 50ºC for 15 seconds, and 60ºC for 4 minutes. The samples were held at 10ºC until ready for processing using the QIAGEN DyeEx 2.0 Spin Kit (QIAGEN #63206). Once the sequencing reactions were dried, they were sent to the University of Florida

Interdisciplinary Center for Biotechnology Research (ICBR) for processing by Sanger sequencing, after which FASTA and fluorescent waveform results were returned. Sequences were verified using BLAST searches against the National Center for Biotechnology Information (NCBI) nucleotide database.

Absolute Quantitative PCR

Fresh cDNA was diluted 10-fold and stored at -20°C for analysis. Both an MJ Research PTC-200 and an Applied Biosystems 7300 real-time PCR machine were used in this study. Reactions were run according to the instructions supplied with the Finnzymes DYNAMO HS 410 SYBR-Green detection system (Fischer #50-995-143). A master-mix was prepared consisting of 10uL DYNAMO reagent, 5.6 uL H_2O, 1 uL 5uM forward + reverse primer and 0.4 uL 50X ROX passive reference dye, each multiplied by n+1 reactions. Each well contained 17 uL of master mix, to which was added 3 uL of template. A standard curve was generated for each gene using amplicon-containing plasmids diluted on a 10-fold gradient from 10^7 through 10^2. The template was either 10-fold-diluted RT reaction (50 ng RT reaction per well), a diluted plasmid standard, or water blank. The reaction components were identical for both machines. See Table 2 for primer annealing temperatures.

The program for thermal cycling was kept constant with the exception of annealing temperature. First samples were warmed to 50°C for 2 minutes, then denatured by 15 minutes at 95°C. Amplification consisted of 40 cycles of denaturation (20 seconds at 95°C), annealing (20 seconds at the primer-specific temperature), and extension (30 seconds at 72°C). One last extension step (10 minutes at 72°C) was run at the end of each reaction. Finally a DNA dissociation curve was generated by ramping the thermocycler temperature from 55°C to 95°C with a plate read every one degree. Each sample, plasmid standard and water blank was run in triplicate to minimize experimental error.

Absolute qPCR data was entered into Microsoft Excel and triplicate results were averaged into single values for each sample. Biological replicates were averaged and graphed including standard error calculations.

Table 2-1. Components of 50mL RNA isolation buffer.

1M Tris-HCl buffer pH 7	5 mL	100 mM
4M NaCL	2.5 mL	200 mM
DL-Dithiothreitol (DTT)	40 mg	5 mM
N-lauroyl sarcosine	500 mg	34 mM
0.5M Ethylenediamine tetraacetic acid	2 mL	20 mM
H_2O treated with 1% Diethylpyrocarbonate (DEPC)	40.5 mL	-

Table 2-2. List of qPCR primers 5' to 3'

Gene	Forward	Reverse	Ta (F)
ZmInCW2	GGTGACCGGGATACAAACGGCACA	GACAAATCCTGCAAATGTCGGGCG	60
ZmSu1	ACCAGAGGATGCAGTCTATG	CCATTCCACTCTGACCAAACG	56
ZmSus2	ACTTTCCACATACCGAGAAGGCCA	AAGGTTTACCAGCTCCCTCAGCTT	56
ZmHXK2	ATAGCAAGCAGAGGGAACTGGGTT	ATCAGCATATCTCCCACCAGCCAA	60
ZmACS2	CCACAGCTCAAACAACTTCACCCT	GTGCTCCGTGGCGAACCT	60
ZmACS6	TGCACTGCACGAGCGGCAA	CGCTCCGTGGCGAACGC	60
ZmACS7	CTCGAACAACTTCACCCTCACCA	CACCAGGTGGATGCCCTTGG	60
ZmERS1-14	ACTCGAGGATGGAAGCCTTGAACT	TCTCCCGTCGGGCAGCAC	60
ZmETR2-9	GCTATGTATGTGTGAAATTTGAGATTAGGA	CTCGTACAAATCTGAGGACGCTCCAG	58
ZmETR2-40	GCTATGTATGTGTGAAATTTGAGATTAGGA	TCAAGTCTGAAGACGCCGCGGAGGAG	57
ZmACO20	CGCCGACGCCGTCATCTT	TCCACGATACACGCATAACCACCGT	60
ZmACO35	CGCCGACGCCGTCATCTT	ACACACATAACTGTGCCACTATAAGCA	56
ZmEIL1-1	GCAGCAGCAGCAGTTCTTCATCC	GTTTATGGCTGGCCGGACATACAAGT	57

CHAPTER 3
RESULTS

The *Mn1* and *mn1* Genotypes

Ethylene Production

A key component of this study was the determination of ethylene generation in developing seeds. GC analysis was performed for two consecutive years, 2007 (Fig. 3-1) and 2008 (Fig. 3-2). Due to differences in kernel physiology, data was plotted on both a nanomols per gram fresh weight (nmol/g/hr) and nanomols per whole kernel basis (nmol/kernel/hr).

Figure 3-1A shows that for the 2007 crop, on a per-gram fresh weight basis, *mn1* produced more ethylene at all stages, with an early peak of ~70 nmol/g/hr at 8 DAP and a maximum rate of 135 nmol/g/hr at 29 DAP. The early peak fell to ~37 nmol/g/hr at 14 DAP before a linear rise to the 29 DAP maximum. The *mn1* ethylene peak at 29 DAP was followed by a steady 85 nmol/g/hr rate through 36 DAP. *Mn1* ethylene production also started with a peak at 8 DAP of over 45 nmol/g/hr, before dropping to half the initial value, remaining constant up to 30 DAP before a sharp increase at 33 DAP that reached over 55 nmol/g/hr. At both 20 and 29 DAP the *mn1* ethylene production was at least 3-fold higher, with an overall hormone peak in *mn1* four days before that shown in *Mn1*.

Figure 3-1B shows the same ethylene data calculated on a per kernel basis. This calculation method highlights the smaller kernel size of the *mn1* genotype due to the *miniature* mutation. The *Mn1* data still showed an initial drop between 8 DAP and 10 DAP, but the starting value of ~3.6 nmol/kernel/hr remained similar between 12 and 20 DAP, reaching ~4 nmol/kernel/hr at this time. The ethylene levels at 33 DAP in *Mn1* rose to over 17.5 nmol/kernel/hr, nearly double the amount in the *mn1* kernels. The *mn1* genotype was similar to *Mn1* in that initial values of ~4 nmol/kernel/hr were more stable before 20 DAP on a per kernel

basis. The 29 DAP peak in *mn1* was still present, but the absolute differences at 20 and 29 DAP were only 50% higher in *mn1* at both time points. It is important to note that where error bars are not shown, the data point was the result of a single biological sample and might not represent the genotype as a whole. Factors that led to the loss of replicate data included technical difficulties with the GC apparatus, poor seed set on pollinated ears, and human error.

During 2008 (Fig. 3-2) *Mn1* and *mn1* samples were more abundant, allowing improved replicate coverage of each time point, especially between 8 and 20 DAP. Figure 3-2A shows that on a per-gram basis the *Mn1* and *mn1* hormone values were similar between 8 and 13 DAP. The *Mn1* ethylene production started at a rate of ~90 nmol/g/hr at 8 DAP, followed by a linear decline to ~28 nmol/g/hr at 20 DAP. This ~28 nmol/g/hr value was maintained for the remainder of observed time points. The *mn1* line had an 8 DAP ethylene production rate of ~70 nmol/g/hr, and after a 20% decrease at 11 DAP, ethylene remained between 45 and 60 nmol/g/hr until 25 DAP, a level nearly twice that of *Mn1*. The *mn1* samples exhibited a 4-fold decrease in ethylene production at 30 DAP versus 25 DAP. When plotted on a per kernel basis (Fig. 3-2B), the *Mn1* genotype produced more ethylene than the *mn1* line at all points tested. This was highlighted by a distinct peak of ethylene in *Mn1* at 13 DAP (~11 nmol/kernel/hr). Hormone levels dropped to ~6.5 nmol/kernel/hr by 16 DAP and remained steady for the remaining time points, with a final measurement of ~4.5 nmol/kernel/hr at 34 DAP. Overall, ethylene production per *mn1* kernel was reduced by 2-fold between 8 and 13 DAP when compared to the wild-type, which remained ~4 nmol/kernel/hr. The *mn1* line showed a ~6 nmol/kernel/hr peak at 16 DAP followed by a gradual downward trend ending at ~4.7 nmol/kernel/hr at 25 DAP. Ethylene levels in *mn1* kernels were below 1 nmol/kernel/hr at 30 DAP, less than half of the wild-type (Fig. 3-2B).

Transcript Accumulation in *Mn1* and *mn1* Genotypes

In order to better understand the relationship between hormone production and kernel physiology, gene expression analysis was performed in order to quantify RNA levels of the genes related to sugar metabolism, ethylene biosynthesis and ethylene perception. Transcript levels were investigated for the following genes: three metabolic genes *Mn1*, *Sus2* and *HXK2*, three ACC synthase genes *ACS2*, *ACS6* and *ACS7*, two ACC oxidase genes *ACO20* and *ACO35*, three ethylene receptors *ERS1-14*, *ETR2-9* and *ETR2-40*, and finally one transcription factor *EIL1-1*. Transcript levels were analyzed using two biological replicates from the 2007 field crop and three replicates from the 2008 crop. All qPCR data from the 2007 harvest were reported as the number of transcripts per nanogram total RNA (# transcripts/ng total RNA). The results from the 2008 crop were reported as both # transcripts/ng total RNA and the number of transcripts per kernel (# transcripts/kernel). In addition, *ACO20*, *ACO35, ETR2-40* and *EIL1-1* were cloned and included in the real-time PCR analysis for year 2008, so year 2007 data for these genes is absent.

Metabolic genes

The causal basis of the *mn1* seed phenotype is the loss of INCW2 enzyme activity, which is encoded by the *Mn1* gene (Cheng et al. 1996).Quantifying this gene provides an internal control for RNA quality and reaction efficiency during sample preparation. Figure 3-3 shows the difference in *Mn1* transcript levels in the *Mn1* and *mn1* lines. The *Mn1* transcript was abundant between 8 and 13 DAP in *Mn1* kernels and reduced by ~95% in the *mn1* background for both 2007 and 2008 samples, correlating with timing of maximum enzyme activity (Chourey et al. 2006). Comparing absolute quantification between year 2007 and year 2008 (Fig. 3-3A and 3-3B, respectively), the 2008 data showed a 50% higher transcript abundance at 8 DAP, reaching ~27,000 transcripts/ng total RNA. At 12 DAP the 2008 samples produced ~9,200 transcripts/ng total RNA, 16% more than year 2007. The transcript levels at later stages were similar between

the years, with ~3,000 transcripts/ng total RNA at 16 DAP and ~1,600 transcripts/ng total RNA at 20 DAP. In Figure 3-3C the trend was similar when calculated per kernel, with peak levels of *Mn1* transcript occurring at 8 DAP at nearly 1.13 x10^9 transcripts/kernel. The only divergence from a steadily downward *Mn1* expression level was at 13 DAP, when # transcripts/kernel showed a slight rise before continuing to recede.

A sucrose synthase gene *Sus2* was chosen as a second internal control (Fig. 3-4). The 2007 results showed very little difference between *Mn1* and *mn1* lines (Fig. 3-4 A), with levels between 600 and 800 transcripts/ng total RNA and sizable standard error at all time points. Figure 3-4B shows the 2008 *Sus2* transcripts/ng total RNA consistently increased over year 2007 amounts, starting with ~1,500 transcripts/ng total RNA at 8 DAP, afterwards increasing in both *Mn1* and *mn1*. In the *Mn1* line, *Sus2* gene peaked at ~3,100 transcripts/ng total RNA by 11 DAP then decreased 20% through 16 DAP before a rise to ~2,700 transcripts/ng total RNA at 20 DAP. The *mn1* line showed a similar trend, with a later, reduced peak of ~2,500 transcripts/ng total RNA at 13 DAP, and a decline to ~1,500 transcripts/ng total RNA for 16 and 20 DAP. On a per kernel basis (Fig. 3-4C) the *Sus2* transcript levels in *Mn1* samples peaked at 13 DAP and remained unchanged thereafter, at ~3x10^8 transcripts/kernel. The *mn1* samples produced a peak *Sus2* transcript level at 11 DAP, two days earlier than *Mn1*, with a noticeable linear decline that ended at 1x10^8 transcripts/kernel at 20 DAP, a value 3-fold lower than *Mn1*.

Hexokinase2 transcript levels (Fig. 3-5) were investigated because members of this gene family are reported to be essential components of sugar sensing and signaling pathways to this study (Saltman 1953; Jang et al. 1997; Yanigisawa et al. 2003). The *HXK2* transcript levels from years 2007 and 2008 showed similarity in the number of transcripts/ng total RNA (Fig. 3-5A and B).Additionally, *HXK2* transcript levels were consistently higher in *Mn1* kernels than the *mn1*.

Figure 3-5A depicts a trend of decreasing expression from 8 to 20 DAP, with an initial transcript level of ~1,500 transcripts/ng total RNA shifting to a final value of ~550 transcripts/ng total RNA in *Mn1* and *mn1* samples. There was no statistically significant difference between the two genotypes tested for that year, although average levels of *HXK2* in *mn1* samples only reached ~70% of the levels in *Mn1*. In Figure 3-5B the *Mn1* value was increased 30% at 8 DAP compared to the same *Mn1* time point for the previous year, but the remaining results for *Mn1* were similar. However, the year 2008 *mn1* data at 8 DAP (~850 transcripts/ng total RNA) showed a 3-fold decrease in transcripts/ng total RNA versus *Mn1* kernels. Figure 5-5B also shows that *HXK2* transcript levels in *mn1* from 13 to 20 DAP were between 50-60% of the related amounts in *Mn1*. Figure 3-5C shows two peaks of *HXK2* transcript accumulation in *Mn1* kernels, the largest at 8 DAP (~1.5x10^8 transcripts/ng total RNA) and another at 13 DAP. There is a 60% decrease overall from 8 to 20 DAP. The *mn1* data showed a constant value for *HXK2* of roughly 3x10^7 transcripts/kernel throughout development. Excluding 13 DAP, *HXK2* transcripts/kernel were at least 3-fold lower in the *mn1* line relative to the wild-type.

The ACC synthase gene family

The ACC synthases catalyze the rate-limiting step in ethylene biosynthesis. Real-time PCR data for the maize ACC synthase family, *ACS2*, *ACS6* and *ACS7* are shown in Figures 3-6 through 3-8, respectively. The expression level of the family as a whole was low, with *ACS2* the most abundant (up to 400 transcripts/ng total RNA), followed by *ACS7*, and *ACS6* appearing as low as 2 and 3 transcripts/ng total RNA (Fig. 3-8). Figure 3-6 reveals subtle variation in *ACS2* transcript between *Mn1* and *mn1* lines, with consistently higher transcript levels in the *Mn1* kernels at 8 DAP. The # of transcripts/ng total RNA in the year 2007 samples (Fig. 3-6A) was approximately half the of those from year 2008 (Fig.3-6B) for both genotypes, but the trends were similar. The *Mn1* kernels showed highest accumulation of *ACS2* at 8 DAP (~400

transcripts/ng total RNA) then dropped over 50% by 12 DAP. The decline continued, with lowest transcript levels at 20 DAP (~75 transcripts/ng total RNA) (Fig. 3-6B). The *mn1* line had transcript levels of ~110 transcripts/ng total RNA at 8 DAP, then showed a relative peak 12-13 DAP. After maximum *ACS2* transcript accumulation of 100 and 200 transcripts/ng in *mn1* at 13 DAP (Fig. 3-6A and B respectively), *ACS2* levels were reduced at 20 DAP. On a per-kernel basis (Fig. 3-6C) the trend for the *ACS2* RNA profile in the *Mn1* samples was more variable, but still showed an overall high-to-low progression between 8 and 20 DAP. Upon calculation of transcript levels per kernel, the 13 DAP peak in *mn1* samples became more prominent (Fig. 3-6).

ACS6 transcripts/ng total RNA in the *Mn1* line (Fig. 3-7A and B) had maxima at 8 DAP followed by progressively lower abundance throughout development, to a 20 DAP value of ~4 transcripts/ng total RNA. The *mn1* line, for the year 2007 crop (Fig. 3-7A), showed peak levels of *ACS6* transcript at 13 DAP, similar to that of *ACS2*. This trend was absent in the 2008 samples (Fig. 3-7B), which instead produced two plateaus, one 8-11 DAP (8 transcripts/ng total RNA) and the second 13-20 DAP (~3 transcripts/ng total RNA). Figure 3-7C shows *ACS6* transcript on a per-kernel basis, which reveals a distinct peak in both *Mn1* and *mn1* lines that was not seen in terms of transcripts/ng total RNA. The *Mn1* line showed no change in transcript amounts at 8 and 11 DAP, then rose to 1.07x10^6 transcripts/kernel at 13 DAP. Following this increase, transcript levels fell to ~5x10^5 transcripts/kernel and remained constant to 20 DAP. In the *mn1* line, *ACS6* increased nearly 2-fold between 8 and 11 DAP, reaching 6.64x10^5 transcripts/kernel. After this 11 DAP peak, transcript levels dropped over 60% by 13 DAP and maintained a consistent level of accumulation through 20 DAP.

The third ACC synthase *ACS7* (Fig. 3-8), showed intermediate levels of transcription compared with the other two family members. Both transcript/ng and transcript/kernel showed

little difference between *Mn1* and *mn1* genotypes with respect to *ACS7*. Figures 3-8A and B demonstrate maximum *ACS7* transcript at 8 DAP for *Mn1* (~60 transcripts/ng total RNA) and *mn1* (~40 transcripts/ng total RNA). Following 8 DAP, transcript levels declined in a linear fashion to final values of ~8-10 transcripts/ng total RNA for both genotypes. Results from year 2007 and year 2008 samples are virtually identical, with similar absolute levels as well as trends. On a per kernel basis (Fig. 3-8C), *Mn1* samples generated a slight peak of *ACS7* transcript at 13 DAP. The *mn1* samples produced maximum *ACS7* transcript levels at 11 DAP, but the difference was not statistically significant. This transcript showed a trend of general decline from 8 to 20 DAP, and both genotypes ended at a final value of ~8x10^5 transcripts/kernel.

The ACC oxidase gene family

Because the ACC synthases catalyze the first step in ethylene biosynthesis, it is important to asses the state of ACC oxidase transcripts in order to represent the final step in ethylene production. Figures 3-9 and 3-10 show results for *ACO20* and *ACO35*, the two ACC oxidase genes investigated in this study. All *ACO* data are from the year 2008 crop. In Figure 3-9A, *ACO20* transcript levels in the *Mn1* genotype remained flat throughout all stages, with a slight decrease between 11 and 13 DAP from ~4,300 to ~3,400 transcripts/ng total RNA. In the same figure *mn1* developed a peak of *ACO20* transcript at 13 DAP of ~5,100 transcripts/ng total RNA, an increase of over 60% versus *Mn1*. The highest expression in *mn1* was ~6,000 transcripts/ng total RNA at 20 DAP, nearly 2-fold higher than *Mn1*. Figure 3-9B demonstrates that on a per kernel basis there was a steady increase in *ACO20* transcript from 8 to 13 DAP in both lines. From 13 to 20 DAP, *ACO20* levels remained unchanged in the wild-type samples at 4x10^8 transcripts/kernel. The *mn1* sample produced 60% of the *ACO20* transcript relative to *Mn1* at 16 DAP, but transcript levels were identical in the two lines at 20 DAP.

The *ACO35* transcript accumulation data (Fig. 3-10) showed similar expression in both *Mn1* and *mn1*. Although *Mn1* produced maximum transcripts/ng total RNA at 8 DAP, and *mn1* produced an *ACO35* peak at 13 DAP, both lines generate approximately 1,000 transcripts/ng total RNA for the first three time points, with similar decreases at 16 and 20 DAP. When calculated on a per kernel basis (Fig. 3-10B), *ACO35* transcript levels were effectively identical between genotypes, with a clear parabolic peak centered on 13 DAP.

The ethylene receptor gene family and *EIL1-1*

Ethylene is perceived by membrane-bound receptors, three of which have been included in this study: *ERS1-14*, *ETR2-9* and *ETR2-40*. The fourth ethylene receptor in maize, *ERS1-25*, is expressed at a lower level than the others (Young and Gallie 2004) and attempts at cloning the gene were unsuccessful during this study. For year 2007 and 2008 samples, the three receptor genes *ERS1-14*, *ETR2-9* and *ETR2-40* were expressed to similar levels, with *ETR2-9* slightly more abundant on a per ng total RNA basis (Figs. 3-11 through 3-13).

For *ERS1-14* in year 2007 samples (Fig. 3-11A) both *Mn1* and *mn1* genotypes produced similar transcript results, with peak accumulation at 8 DAP (~560 transcripts/ng total RNA). After a drop to ~300 transcripts/ng total RNA at 12 DAP, subsequent time points remained consistent ending with ~250 transcripts/ng total RNA at 20 DAP. Results from the year 2008 samples (Fig. 3-11B) showed an increase of ~20% over year 2007 data. However, the trend for *Mn1* kernels was similar, with an 8 DAP peak of 630 transcripts/ng total RNA followed by a 30% decline at 11 DAP, remaining constant thereafter. The *mn1* kernels from year 2008 diverged from the previous year's results, with 8 DAP *ERS1-14* levels that started at ~530 transcript/ng, then increased 10% to peak at 11 DAP, generating 50% more transcript than *Mn1* at that time point (Fig. 3-11B). After the 11 DAP peak, *ERS1-14* levels in *mn1* returned to wild-type levels at 16 and 20 DAP. The peak in *ERS1-14* transcripts at 11 DAP was visible on a per kernel basis as

well (Fig. 3-11C), marking the only point that *mn1* demonstrated higher values than *Mn1*. Both genotypes showed identical plateaus from 13 to 20 DAP, though *ERS1-14* transcripts/kernel were insignificantly lower in m*n1-1* than *Mn1*.

Figure 3-12 shows the transcript results for the most abundant receptor, *ETR2*-9. Year 2007 samples produced an identical profile of *ETR2-9* generation between *Mn1* and *mn1*, decreasing from ~860 transcripts/ng total RNA at 8 DAP to just over 500 transcripts/ng total RNA at 20 DAP (Fig. 3-12A). No statistically significant differences were observed. Figure 3-12B shows data from the 2008 harvest on a per ng total RNA basis. A similar trend emerged as in the previous year; *ETR2-9* transcript declined as development progressed. In addition, the accelerated decline of *ETR2-9* transcript in *mn1* samples was significant at 13 DAP, when *mn1* kernels produced only 65% of the *ETR2-9* transcript versus the wild-type. This observation is supported on a per kernel basis by the results shown in Figure 3-12C. Both genotypes produced a similar 2-fold transcript increase from 8 to 11 DAP, after which the two lines diverged: The *Mn1* samples generated ~8x10^7 transcripts/kernel at 13 DAP, roughly 3-fold higher than *mn1*. The wild-type kernels subsequently maintained at least 50% higher *ETR2-9* transcripts/kernel at 16 and 20 DAP.

Figure 3-13A depicts year 2008 results for *ETR2-40*, showing a ~646 transcript/ng peak in the *Mn1* kernels at 8 DAP that was not reflected in *mn1* samples. Other than this difference, both genotypes produced no significant variation in amounts of transcript, remaining between 300 and 350 transcripts/ng total RNA from 11 to 20 DAP. Per kernel results for *ETR2-40* (Fig. 3-13B) showed an increase in both genotypes from 8 to 11 DAP. At 13 DAP, the *Mn1* samples showed increased transcript accumulation of ~4x10^7 transcripts/kernel and maintained that level for the

remaining time points. At 13 DAP the *mn1* kernels decreased accumulation to ~2.23x10^7 transcripts/kernel through 20 DAP, 2-fold lower than *Mn1* results.

The transcription factors *EIN3* and *EIL1* are downstream transducers of ethylene perception. *EIL1-1* was included in this study as a representative of this group of genes (Fig. 3-14). For both *Mn1* and *mn1* samples, *EIL1-1* exhibited the trend of showing lowest transcript levels at 8 DAP and steadily rising to a peak at the latest stage measured, 20 DAP. Figure 3-14A shows *Mn1* remained constant from 8 to 16 DAP, maintaining 740-780 transcripts/ng total RNA. Over the same period *mn1* samples produced a peak of *EIL1-1* transcript accumulation at 13 DAP ~30% higher than the *Mn1* kernels. Both lines eventually rose to their maximum values of 1,200 transcripts/ng total RNA at 20 DAP. On a per kernel basis (Fig. 3-14B) the two lines produced similar increases in *EIL1-1* transcript during development. From 13 to 16 DAP, *Mn1* transcript production was unchanged (~9.2x10^7 transcripts/kernel) but the *mn1* line decreased temporarily at 16 DAP to 4.89x10^7 transcripts/kernel. The subsequent increase at 20 DAP was proportionally similar between genotypes, but the *Mn1* value of 1.35x10^8 transcripts/kernel at 20 DAP was ~30% higher than *mn1* at the same time point.

The *Su1* and *su1* Genotypes

Ethylene Production

The *Su1* and *su1* genotypes were included in this study in order to provide data for a late-acting starch synthesis mutation, as compared to the *mn1* seed mutation that affects carbohydrate metabolism during the early stages of seed development. The ethylene production results for the *Su1* and *su1* genotypes were reported using the same convention as the *Mn1* and *mn1* data. Figure 3-15 shows ethylene production for the year 2007 samples. On a per gram fresh weight basis (Fig. 3-15A) both genotypes produced ~35 nmol/g/hr ethylene at 12 DAP, the highest amount in either line for all time points tested. There was a ~40% decline in ethylene at 16 DAP

in both lines. At 20 DAP *su1* kernels produced 27 nmol/g/hr ethylene, 50% more than *Su1* seeds. Both lines reached their lowest production rate, ~11 nmol/g/hr, at 28 DAP. Figure 3-15B shows results in terms of # nmol/kernel/hr, revealing a decrease in ethylene production for both genotypes from 8-16 DAP. The *Su1* kernels produced a minor peak of ~5.5 nmol/kernel/hr at 12 DAP and a major peak of 8 nmol/kernel/hr at 24 DAP. The ethylene level in the *su1* mutant at 12 DAP was similar to that in the wild-type, as was the subsequent decrease at 16 DAP and rise to ~7 nmol/kernel at 20 DAP. Due to technical difficulties the data for *su1* kernels at 24 DAP were not recovered. At 28 DAP the results of 4.5 nmol/kernel/hr for *Su1* and *su1* kernels were similar, showing a downward trend at this stage in both lines.

During 2008, the *Su1* line grew abundantly, providing excellent coverage of all time points. The *su1* mutant line, however, showed poor germination, allowing only one or two replicates per stage. Bars represent standard error of between two and four biological replicates for *Su1* and two replicates for *su1*. Figure 3-15A shows that the highest level of ethylene production was at the earliest time point sampled for both *Su1* (~45 nmol/g/hr, 8 DAP) and *su1* (~40 nmol/g/hr, 12 DAP). Hormone levels dropped sharply in *Su1* from 20 nmol/g/hr at 12 DAP to 10 nmol/hr at 20 DAP. There was a slight increase of ethylene 20-25 DAP before production reached the observed minimum of ~2 nmol/g/hr from 28-30 DAP. This lowest value in *Su1* kernels was followed by a rise to ~5 nmol/g/hr at 34 and 37 DAP. The *su1* line produced a similar trend as *Su1*, decreasing 3-fold from 12 to 20 DAP. The *su1* minimum value was slightly earlier than the wild-type but similar in rate (~2 nmol/g/hr). As in the *Su1* samples, ethylene production showed an upward trend at 35 DAP. When considered on a per kernel basis (Fig. 3-16B), the *Su1* kernels did not have a maximum at 8 DAP, but instead produced distinct peaks above 4 nmol/kernel/hr at 16 and 24-25 DAP. The timing of the later peak corresponded well

with 2007 observations (Fig. 3-15B and 3-16B). Later development showed similar trends as the per gram results, with a minimum at 28-30 DAP followed by a ~2-fold increase at 34-37 DAP. The *su1* mutant kernels generated more ethylene than wild-type at 12 and 14 DAP but fell more sharply at 20 and 25 DAP, preceding both the initial peak and initial decline of the wild-type by ~5 days. The *su1* samples showed an increasing trend late in development that resembled *Su1* kernels, and reached a 2 nmol/kernel/hr rate at 35 DAP.

Transcript Accumulation in *Su1* and *su1* Genotypes

Due to difficulties in generating complete time courses for *Su1* and *su1* genotypes, each of the data points representing transcript levels were derived from single biological samples. Less emphasis will be placed on slight differences in transcript levels because of the questionable reproducibility of the results. Error bars represent experimental error for the real-time PCR reactions.

Metabolic genes

The *Su1* transcript was used as an internal control for RNA quality and reaction efficiency during qPCR sample preparation. This was due to the published similarity in S*u1* transcript levels in *Su1* and *su1* genotypes (Dinges et al. 2001). Samples from each year demonstrated little difference in transcript level between mutant and wild-type lines on a per ng total RNA basis (Fig. 3-17A and B). The highest observed transcript levels were at the 12-14 DAP stage for both years followed by a 3-fold decline as development progressed. In the year 2007 samples, 12 DAP results showed ~8x10^3 transcripts/ng total RNA, and there was a second minor peak at 20 DAP (~5.5x10^3 transcripts/ng total RNA) before the downward trend resumed, which caused the *Su1* and *su1* transcript levels to mirror trends in ethylene production (Fig. 3-16). For year 2008 samples, # transcripts on both a per ng total RNA and per kernel basis dropped steadily from early to late development. A delay in transcript reduction in the *Su1* genotype caused 2-fold

higher accumulation at 20 DAP over levels in the *su1* mutant. Absolute amounts of *Su1* transcript were shown to be three-fold lower in the 2008 crop, which produced from 2,500 to 500 transcripts/ng total RNA between 14 and 35 DAP.

The gene *Sus2* encodes a member of the sucrose synthase family, which catalyzes the unidirectional cleavage of sucrose into fructose and UDP-glucose. In Figure 3-18, *Sus2* transcript accumulation is shown to vary between year 2007 and 2008 samples. In the *Su1* kernels, for year 2007 (Fig. 3-18A), *Sus2* transcript was lowest at 8 DAP then had a peak of ~1,700 transcripts/ng total RNA at 12 DAP. After this time point, transcript levels dropped 40% at 16 DAP then reached their maximum level of 2,500 transcripts/ng total RNA at 20 DAP. Finally, *Sus2* levels declined to ~1,400 transcripts/ng total RNA at 28 DAP. The *su1* kernels showed an upward trend at 8 and 12 DAP, similar to wild-type, but generated a peak 4 days earlier at 16 DAP (~2,250 transcripts/ng total RNA). After this peak, *Sus2* levels remained between 1,500 and 1,800 transcripts/ng total RNA for the rest of development. The *Su1* and *su1* samples from year 2008 showed similar trends when compared by # transcripts/ng total RNA as well as # transcripts/kernel (Fig. 3-17 B and C). In *Su1* seeds the *Sus2* transcript level was elevated 2-fold over that of *su1* samples. The trend for *Sus2* showed consistent levels of accumulation throughout development. *Su1* kernels maintained between 2,000 and 2,500 transcripts/ng total RNA, and *su1* produced over 1,000 transcripts/ng total RNA at all time points. Figure 3-17C shows the same 2-fold increase in *Sus2* transcript in the wild-type samples (~2x10^8 transcripts/kernel) over those in the *su1* mutant (~1x10^8 transcripts/kernel) at all stages. At 35 DAP, the *Su1* sample reached a peak of 2.67x10^8 *Sus2* transcripts/kernel.

Another sugar-related transcript, *HXK2*, showed consistent patterns of accumulation between years and genotypes. The highest transcript accumulation, 1,500-1,800 transcripts/ng

total RNA, was from 12-15 DAP, and decreased as development progressed (Fig. 3-19A and B). For year 2007 samples, there was a 2.5-fold higher peak at 8 DAP in the *su1* sample that was not present during the following year. Figure 3-19C shows that, on a per kernel basis, both genotypes underwent steady decline in *HXK2* transcript levels from an initial peak of ~1.5x10^8 transcripts/kernel at 14 DAP. The *Su1* kernels showed a 2-fold higher *HXK2* transcript level than *su1* kernels at 20 DAP. By 25 DAP the two genotypes contained similar amounts of transcript (~5x10^7 transcripts/kernel) that was unchanged for the remainder of development.

The ACC synthase gene family

The ACC synthase enzymes catalyze the first committed step in ethylene biosynthesis (Yang and Hoffman 1984). The ACC synthase gene family retained a similar distribution as that seen in *Mn1* and *mn1* kernels, in that *ACS* transcripts were comprised mainly of *ACS7* and *ACS2*, followed by a 2-fold less *ACS6* (Figs. 3-20 to 3-22). Figure 3-20A contains year 2007 data for *ACS2*, showing peaks of 100 transcripts/ng total RNA at 12 and 20 DAP in the *Su1* line. Between these peaks were intervening lows of ~25 transcripts/ng total RNA at 16 and 28 DAP. The *su1* samples were expressed at ~35 transcripts/ng total RNA between 12 and 20 DAP. The maximum expression levels were at the first and last stages tested; first over 450 transcripts/ng total RNA at 8 DAP and last 3-fold lower at 28 DAP. The kernels from year 2008 (Fig. 3-20B and C) showed reduced *ACS2* transcript levels compared to year 2007, with expression under 50 transcripts/ng total RNA for 14 and 20 DAP. Both genotypes produced rising levels of transcript as development progressed. *Su1* kernels produced 2-fold more *ACS2* at 25 and 35 DAP. The maximum transcript levels were at 35 DAP, of 150 transcripts/ng total RNA for *Su1* kernels and 72 transcripts/ng total RNA for *su1*.

ACS6 was the least-expressed member of this gene family (Fig. 3-21). All three plots of transcript accumulation showed highest levels before 15 DAP for both *Su1* and *su1* lines. During

year 2007 (Fig. 3-21A) *Su1* seeds produced less than 4 transcripts/ng total RNA at 8 DAP, 6-fold lower than *su1*. All *Su1* results from this year showed less than 10 transcripts/ng total RNA, with a steadily decreasing trend after 12 DAP. The *su1* line produced a clear maximum *ACS6* transcript accumulation at 8 DAP, then showed consistently lower amounts from 12-28 DAP (~6 transcripts/ng total RNA). The year 2008 samples showed highly similar distributions of transcript in both *Su1* and *su1* kernels (Fig. 3-21B). The highest levels for both lines were again at the earliest point assessed; 20-25 transcripts/ng total RNA at 14 DAP. *ACS6* accumulation dropped to ~8 transcripts/ng total RNA at 25 DAP, and continued at this level through 35 DAP. When calculated on a per kernel basis (Fig. 3-21C), the *Su1* genotype maintained a high level of *ACS6* transcript at 14 and 20 DAP, ~ 2.5x10^6 transcripts/kernel. In contrast, *su1* kernels showed a 2-fold decrease of *ACS6* transcript between 14 and 20 DAP. For each time point from 25 to 35 DAP, both lines generated ~7x10^5 transcripts/kernel.

The third ACC synthase gene, *ACS7*, was the highest-expressed member of the family in *Su1* and *su1* genotypes (Fig. 3-22). For year 2007, results indicated constant expression, between 100 and 200 transcripts/ng total RNA, from 12 through 28 DAP (Fig. 3-22A).In *su1* samples there was a 2-fold higher accumulation at 8 DAP, and in *Su1* samples the transcript level dropped sharply at 28 DAP (24 transcripts/ng total RNA). Figure 3-22B shows that the 2008 samples had lower absolute levels of *ACS7* transcript than year 2007, and maintained 50-125 transcripts/ng total RNA for all time points. These samples produced no peaks, which led to constant *ACS7* levels in both genotypes from 14 through 35 DAP. When calculated on a per kernel basis (Fig. 3-22C), both *Su1* and *su1* genotypes had highest *ACS7* accumulation at 14 DAP, greater than 1x10^7 transcripts/kernel. Both lines' transcript levels fell to ~6x10^6 transcripts/kernel at 20 DAP. *Su1* samples maintained this amount until 30 DAP, then produced a

peak of 1x10^7 transcripts/kernel at 35 DAP. The *su1* line had a slight downward trend from 20 to 35 DAP, ending at 5x10^6 transcripts/kernel.

The ACC oxidase gene family

ACC oxidase enzymes catalyze the final step in ethylene biosynthesis. Figure 3-23 shows transcript levels of *ACO20* in the year 2008 field samples. Both *Su1* and *su1* genotypes produced ~1,200 transcripts/ng total RNA at 14 DAP (Fig. 3-23A). There was a peak of nearly 2,000 transcripts/ng total RNA in *su1* samples at 20 DAP, a 50% higher transcript accumulation than the *Su1* line. At 25 DAP both genotypes returned to parallel levels of 1,600 transcripts/ng total RNA. After this time point there was a decrease in *ACO20* transcript levels in all samples that ended with 1,000 and 1,200 transcripts/ng total RNA at 35 DAP for *Su1* and *su1*, respectively. When data was calculated on a per kernel basis, both lines produced ~1.2x10^8 transcripts/kernel at all stages, with the exception of 20 DAP peaks of 1.83x10^8 transcripts/kernel in *Su1* and 1.5x10^8 transcripts/kernel in *su1* (Fig. 3-23B).

For the *ACO35* gene (Fig. 3-24), transcript levels in *Su1* kernels increased from 500 transcripts/ng total RNA between 14 and 20 DAP to a peak of ~1,750 transcripts/ng total RNA by 35 DAP. The *su1* line also produced ~500 transcripts/ng total RNA from 14 to 20 DAP, but had a smaller increase over time, reaching ~900 transcripts/ng total RNA at 30 and 35 DAP. When calculated on a per kernel basis, the trend remained consistent, with increasing transcript accumulation from 5x10^7 transcripts/kernel at 15 DAP to 7.5x10^7 transcripts/kernel at 30 DAP (Fig. 3-24B). From 30 to 35 DAP the *Su1* line produced a 2-fold higher accumulation of *ACO35* transcript. However, in the *su1* line transcript levels remained constant from 30 to 35 DAP, 65% lower than wild-type.

The ethylene receptor gene family and *EIL1-1*

Ethylene receptors are the initial point of ethylene perception in plants. Three ethylene receptor genes, *ERS1-14*, *ETR2-9* and *ETR2-40*, were quantified in the *Su1* and *su1* developmental series. Figure 3-25 shows *ERS1-14* levels for kernels from both 2007 and 2008 field harvests. For year 2007 samples (Fig. 3-25A) accumulation was between 200 and 360 transcripts/ng total RNA for both genotypes throughout development, with the exception of *su1* kernels, which contained over 800 transcripts/ng total RNA at 8 DAP. Data from year 2008 samples (Fig. 3-25B) showed similar amounts of *ERS1-14* accumulation as the previous year. Both *Su1* and *su1* series experienced a 50% decrease in transcript amount from 14 to 35 DAP. The *Su1* line produced ~450 transcripts/ng total RNA at 8 DAP; 40% more than *su1* kernels at the same stage. This 40% higher *ERS1-14* transcript accumulation occurred at all time points except 30 DAP, at which point the results for the two genotypes were identical. Figure 3-25C shows that the *Su1* series produced a peak of 4.5x10^7 transcripts/kernel at 20 DAP and a low of 1.5x10^7 transcripts/kernel at 30 DAP, before a final increase to 3x10^7 transcripts/kernel. In *su1* kernels the *ERS1-14* transcript levels were highest at 8 DAP, accumulating to 3x10^7 transcripts/kernel. By 20 DAP abundance had dropped to 1.6x10^7 transcripts/kernel, 3-fold lower than wild-type, and remained constant through 35 DAP.

As in the *Mn1* and *mn1* samples, *ETR2-9* was the most abundant receptor transcript, with up to 10-fold higher levels than the other two family members (Fig. 3-26). The results from the year 2007 harvest resembled the figure for ethylene production (Figs.3-15 and 3-26A), with two peaks clearly defined in both genotypes; ~800 transcripts/ng total RNA at 12 DAP and ~650 transcripts/ng total RNA at 20 DAP. Both lines showed decreased accumulation of *ETR2*-9 transcript at 28 DAP (~325 transcripts/ng total RNA). For year 2008 samples (Fig. 3-26B), transcript levels were 5-fold higher than those from the previous year. *ETR2-9* decreased in

nearly linear fashion throughout development of both genotypes, from over 3,500 transcripts/ng total RNA at 14 DAP to ~2,000 transcripts/ng total RNA at 35 DAP. Figure 3-26C demonstrates peaks of *ETR2-9* in the *Su1* samples at 20 and 35 DAP, similar to *ERS1-14* transcript (Fig. 3-25C). Levels in *Su1* kernels were 2-fold higher than *su1* kernels at 20 DAP. Results for *ETR2-9* transcript levels in *su1* kernels showed highest levels at 14 DAP (3.5x10^8 transcripts/kernel), which decreased to 2x10^8 transcripts/kernel at 20 DAP and ~1.3x10^8 transcripts/kernel at 35 DAP.

For *ETR2-40* (Fig. 3-27), the data did not correlate to the other two receptor trends, with transcript levels in *Su1* samples higher at 14 DAP but lower at 30 DAP as a portion of total RNA (Fig. 3-27A). *ETR2-40* transcripts in *Su1* kernels decreased in a linear fashion from ~175 transcripts/ng total RNA at 14 DAP to ~80 transcripts/ng total RNA at 30 DAP. There was an upward trend at 35 DAP (~140 transcripts/ng total RNA). The *su1* line displayed an increasing level of *ETR2-40* transcript from 100 transcripts/ng total RNA at 14 DAP to ~145 transcripts/ng total RNA at 30 and 35 DAP. Per kernel (Fig. 3-27C), *ETR2-40* transcript levels displayed the same peak in 20 DAP *Su1* kernels that was seen for *ERS1-14* and *ETR2-9* transcripts. This peak reached ~2x10^7 transcripts/kernel and was followed by a decrease in transcript accumulation at 30 DAP, as well as a secondary peak at 35 DAP that paralleled trends in the other receptor transcript levels. The *su1* results for *ETR2-40* showed an overall increase during development, from below 1x10^7 transcripts/kernel during early stages to ~1.2x10^7 transcripts/kernel by 35 DAP. Both *ERS1-14* and *ETR2-9* decreased during the same period (Figs. 3-25C and 3-26C).

Levels of *EIL1-1* transcript from year 2008 samples are shown in Figure 3-28. For *Su1* kernels, transcript levels were between 700 and 800 transcripts/ng total RNA at 14, 20, and 30 DAP (Fig. 3-28A). These points were separated by peaks of ~1,250 transcripts/ng total RNA at

25 and 35 DAP. For *su1* samples, there was a decrease from ~1,140 transcripts/ng total RNA at 14 DAP to ~860 transcripts/ng total RNA at 25 DAP. By 30 DAP *EIL1-1* transcript levels peaked in *su1* at ~1,200 transcripts/ng total RNA, and produced a similar amount at 35 DAP as well. Upon calculation of transcript amounts per kernel, observations remained unchanged. Figure 3-28B shows that *EIL1-1* accumulation in *Su1* kernels increased after 14 DAP to a plateau of ~1x10^8 transcripts/kernel from 20-25 DAP. This amount was decreased 50% at 30 DAP, then rose to 1.5x10^8 transcripts/kernel at 35 DAP. In *su1* samples the maximum transcript accumulation was over 1x10^8 transcripts/kernel at 14 and 35 DAP, with a minimum value, ~6.3 transcripts/kernel, at 25 DAP.

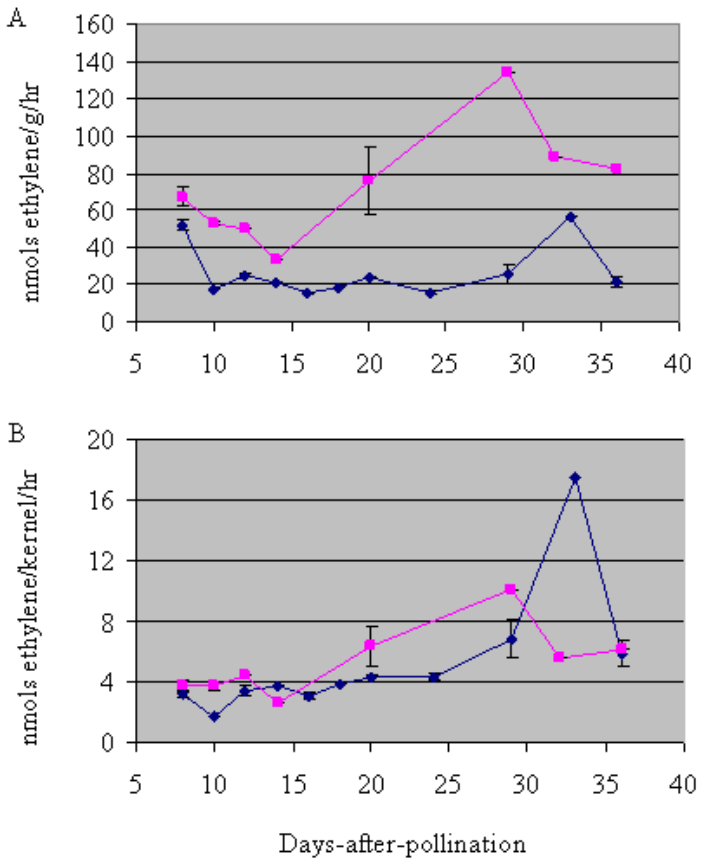

Figure 3-1. Ethylene produced by *Mn1* (blue) and *mn1* (pink) kernels, nmols of A) nmol/g/hour B) nmol/kernel/hour (Summer 2007 field harvest)

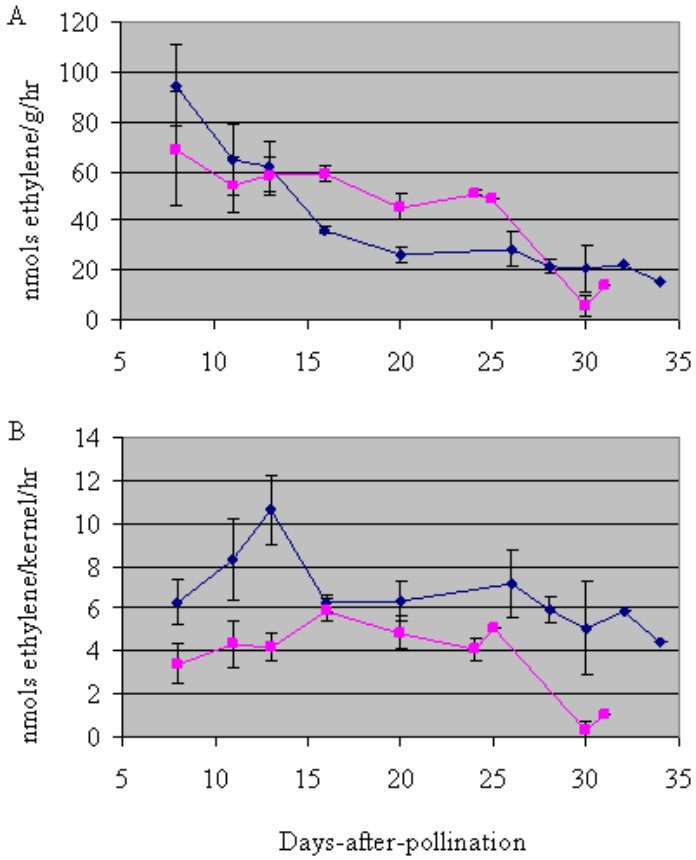

Figure 3-2. Ethylene produced by *Mn1* (blue) and *mn1* (pink) kernels, nmols of A) nmol/g/hour B) nmol/kernel/hour (Summer 2008 field harvest)

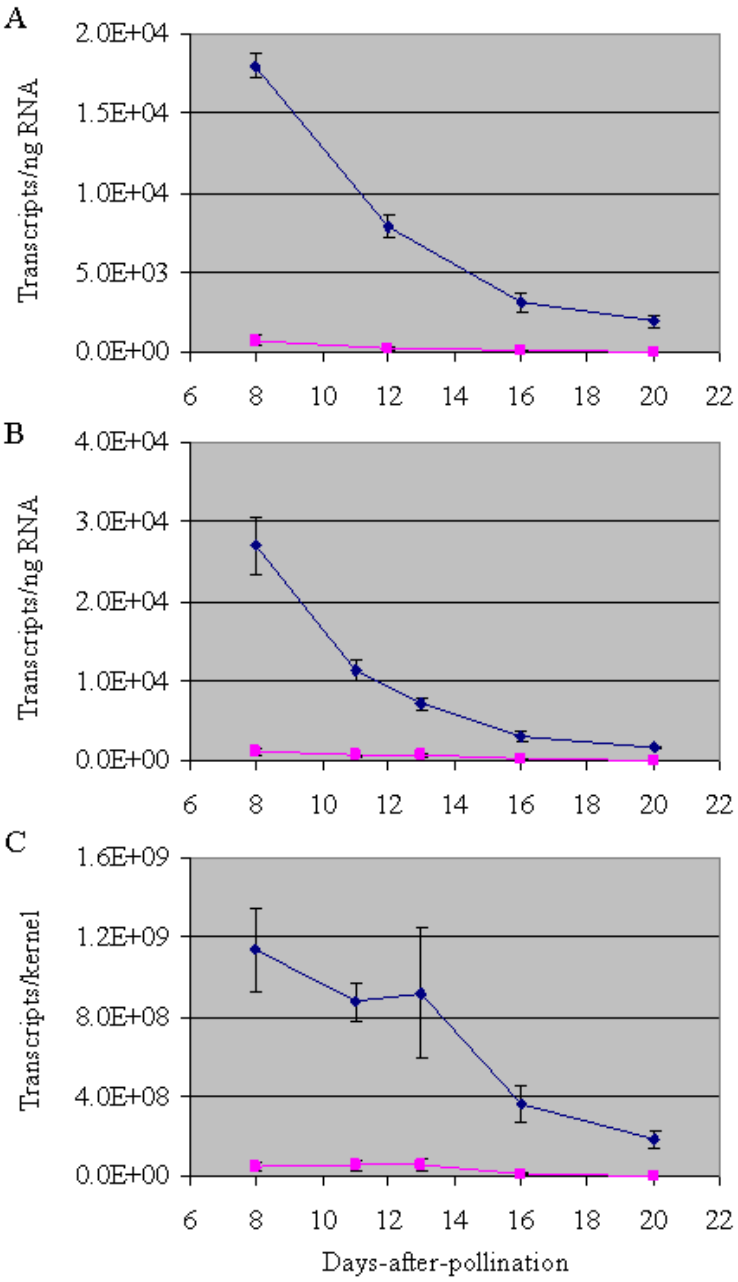

Figure 3-3. *Mn1* transcript levels in *Mn1* (blue) and *mn1* (pink) kernels A) transcripts per nanogram RNA (Summer 2007 samples) B) transcripts per ng RNA (Summer 2008 samples) C) transcripts per kernel (Summer 2008 samples)

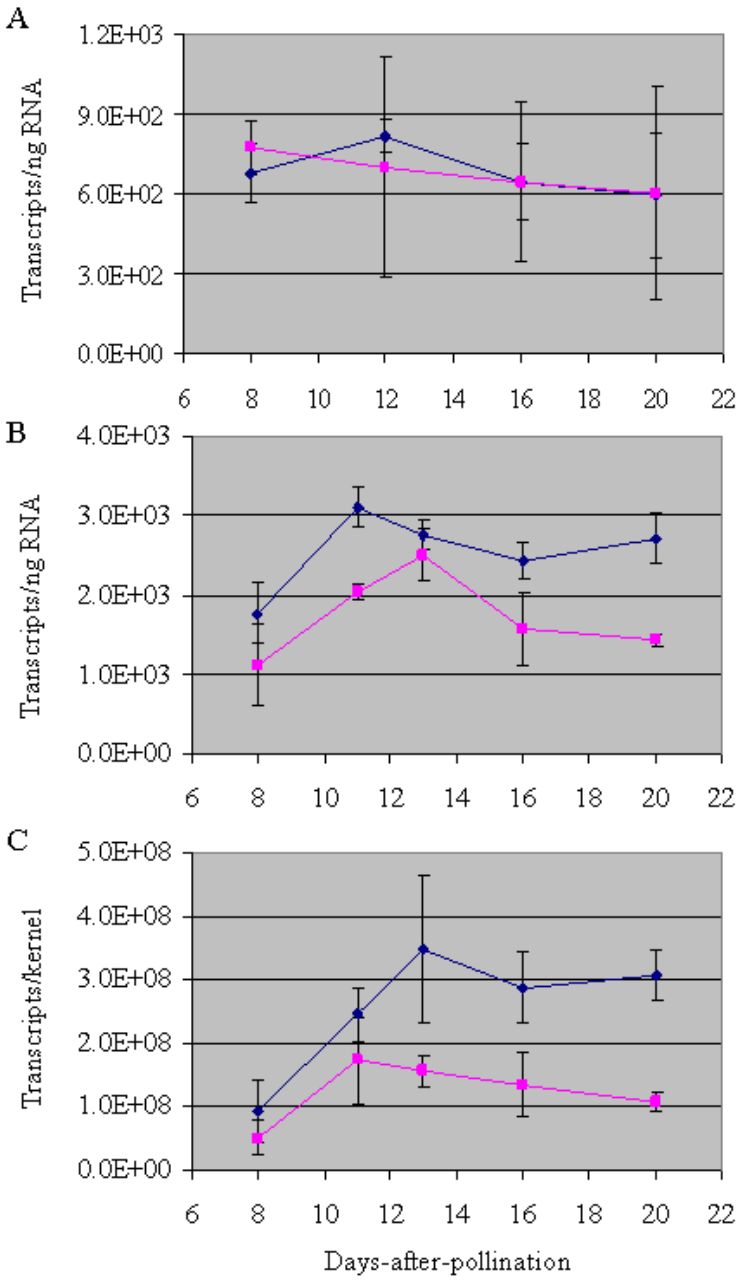

Figure 3-4. *Sus2* transcript levels in *Mn1* (blue) and *mn1* (pink) kernels A) transcripts per nanogram RNA (Summer 2007 samples) B) transcripts per ng RNA (Summer 2008 samples) C) transcripts per kernel (Summer 2008 samples)

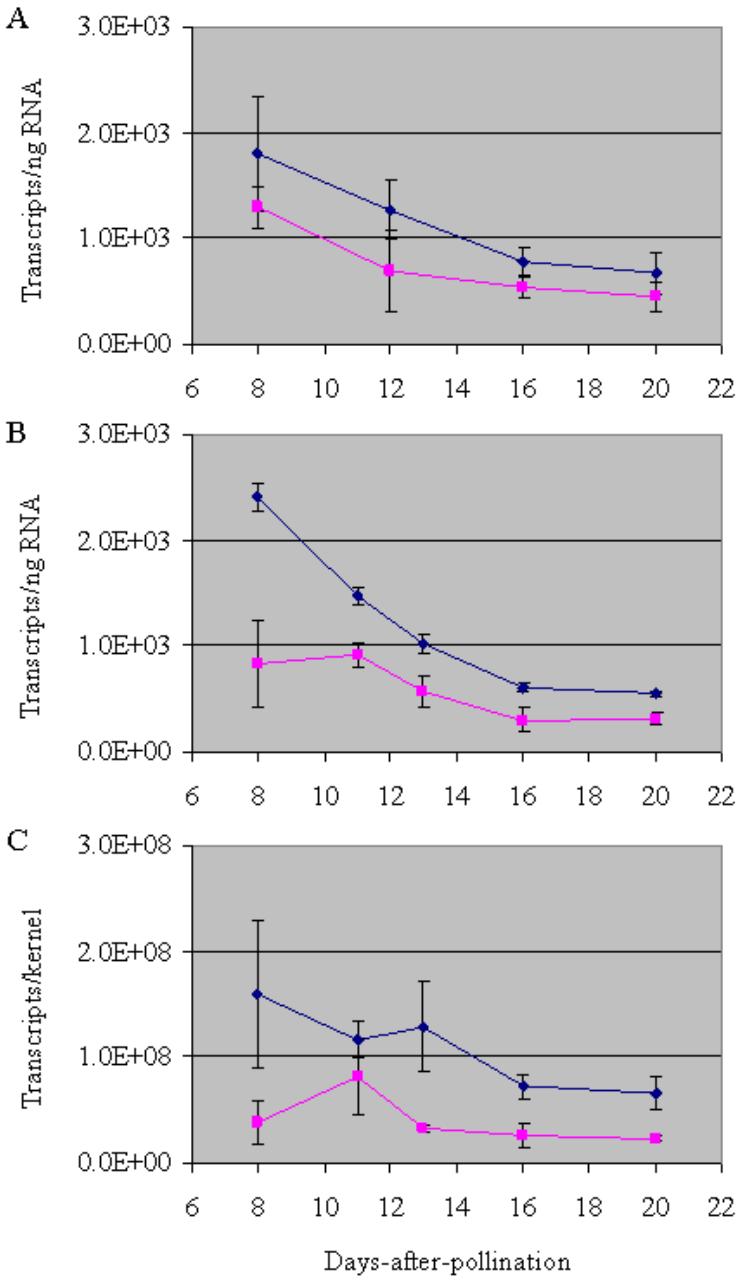

Figure 3-5. *HXK2* transcript levels in *Mn1* (blue) and *mn1* (pink) kernels A) transcripts per nanogram RNA (Summer 2007 samples) B) transcripts per ng RNA (Summer 2008 samples) C) transcripts per kernel (Summer 2008 samples)

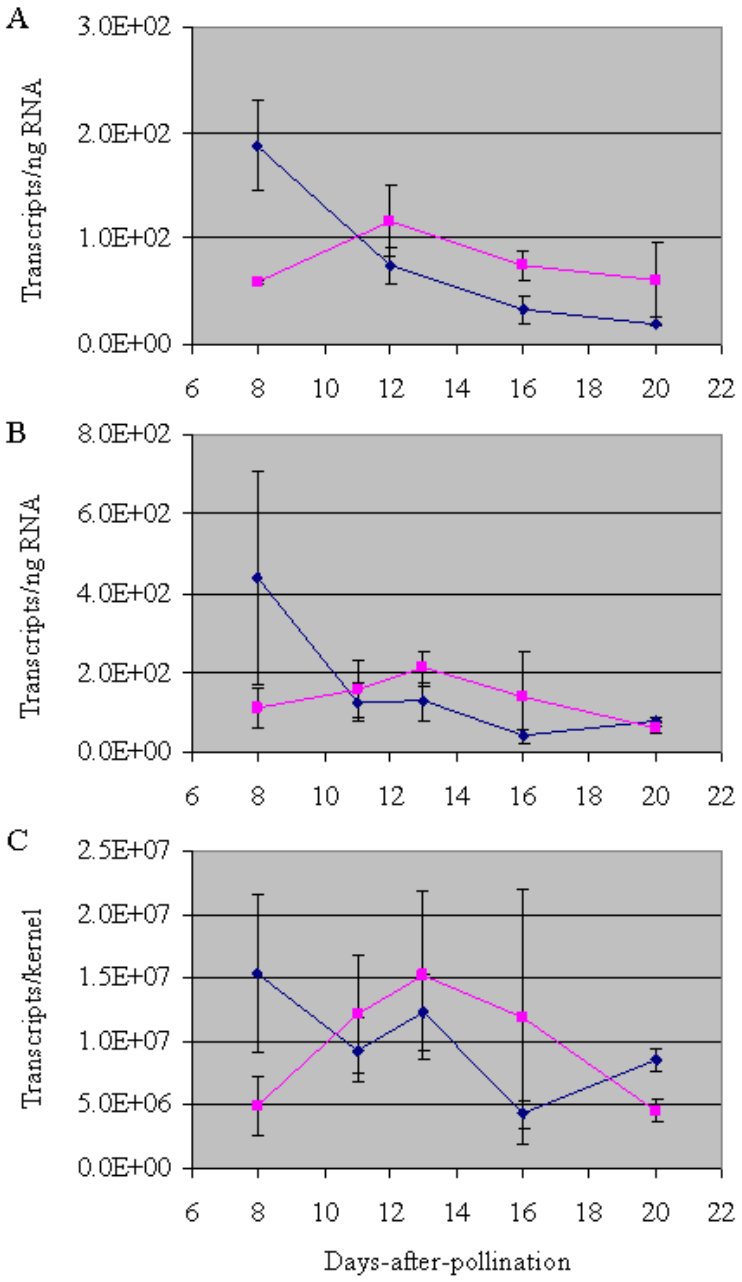

Figure 3-6. *ACS2* transcript levels in *Mn1* (blue) and *mn1* (pink) kernels A) transcripts per nanogram RNA (Summer 2007 samples) B) transcripts per ng RNA (Summer 2008 samples) C) transcripts per kernel (Summer 2008 samples)

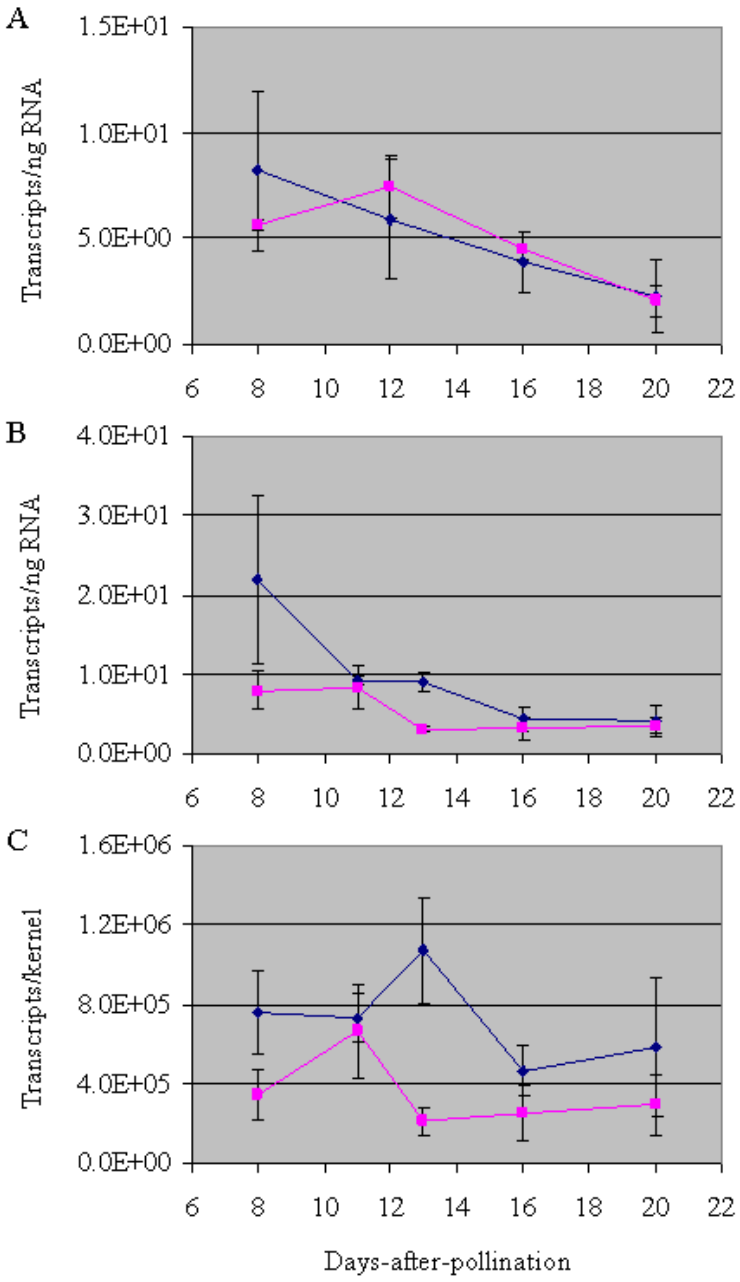

Figure 3-7. *ACS6* transcript levels in *Mn1* (blue) and *mn1* (pink) kernels A) transcripts per nanogram RNA (Summer 2007 samples) B) transcripts per ng RNA (Summer 2008 samples) C) transcripts per kernel (Summer 2008 samples)

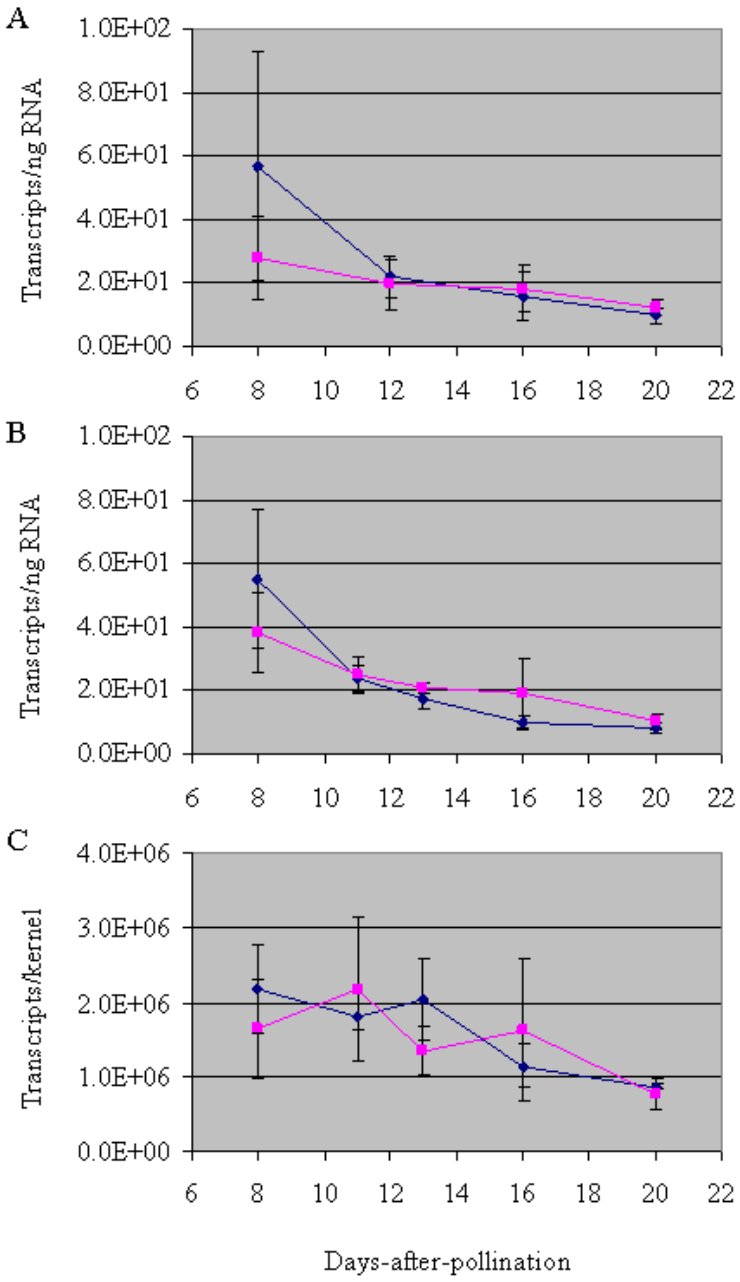

Figure 3-8. *ACS7* transcript levels in *Mn1* (blue) and *mn1* (pink) kernels A) transcripts per nanogram RNA (Summer 2007 samples) B) transcripts per ng RNA (Summer 2008 samples) C) transcripts per kernel (Summer 2008 samples)

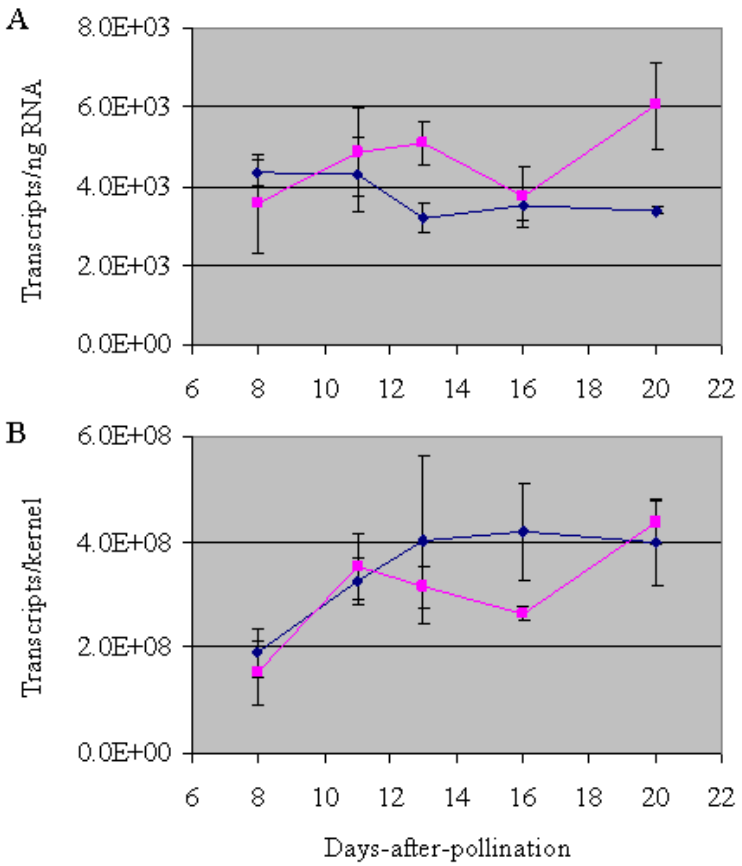

Figure 3-9. *ACO20* transcript levels in *Mn1* (blue) and *mn1* (pink) kernels (Summer 2008 samples) A) transcripts per nanogram RNA B) transcripts per kernel

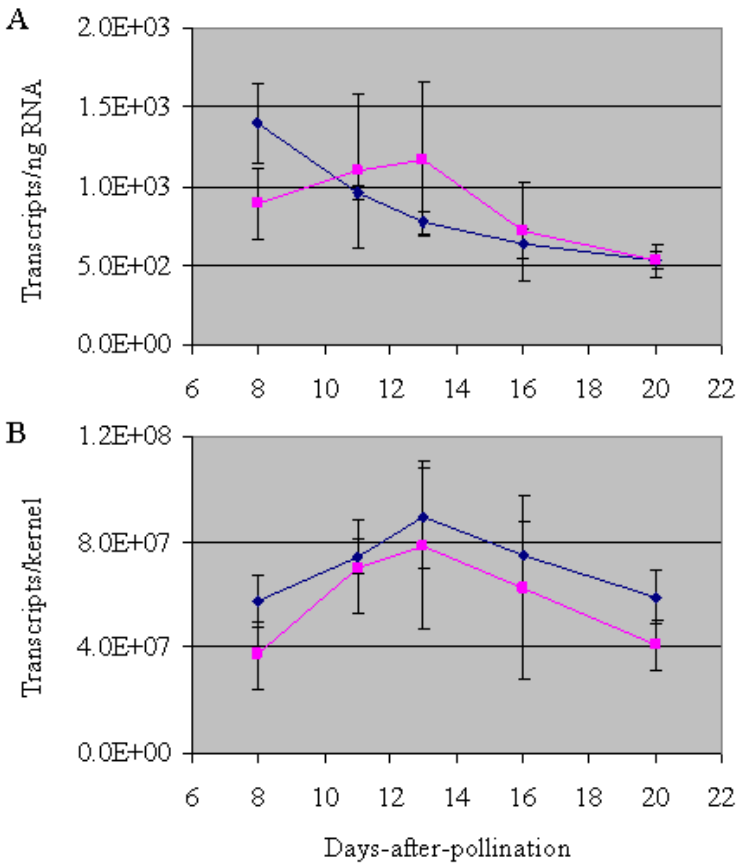

Figure 3-10. *ACO35* transcript levels in *Mn1* (blue) and *mn1* (pink) kernels (Summer 2008 samples) A) transcripts per nanogram RNA B) transcripts per kernel

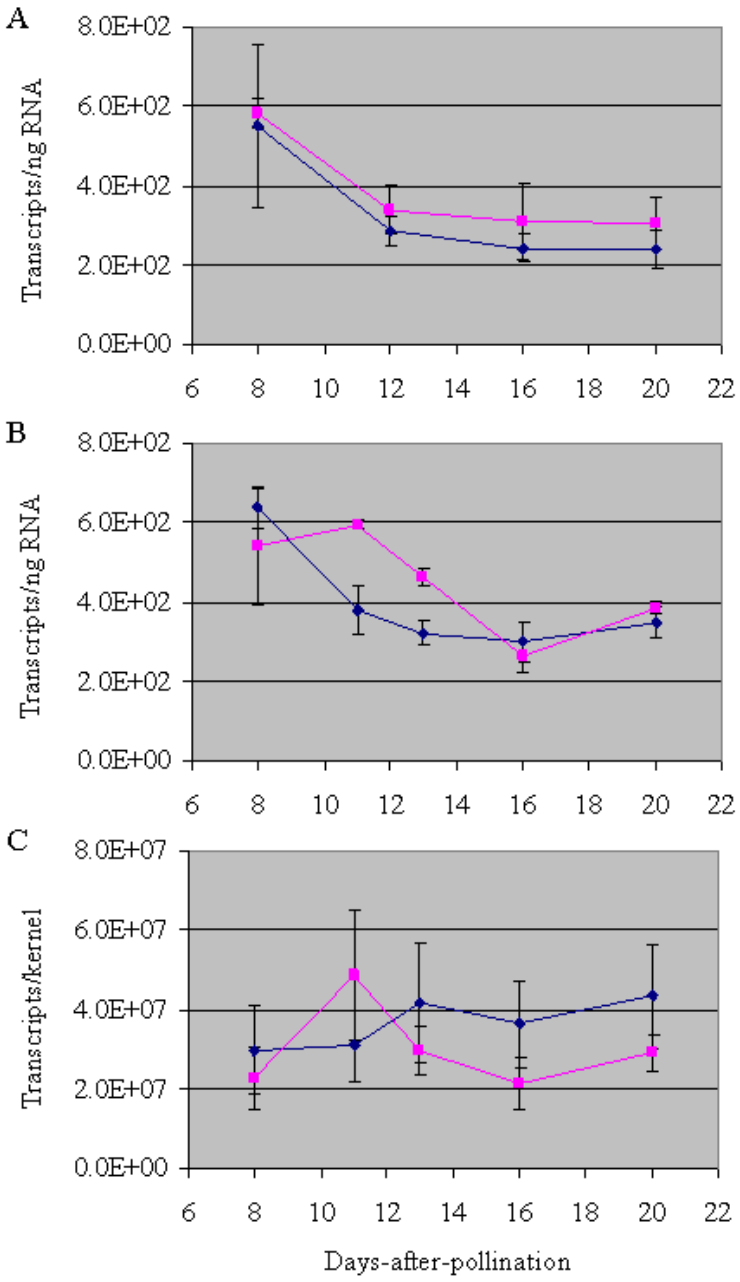

Figure 3-11. *ERS1-14* transcript levels in *Mn1* (blue) and *mn1* (pink) kernels A) transcripts per nanogram RNA (Summer 2007 samples) B) transcripts per ng RNA (Summer 2008 samples) C) transcripts per kernel (Summer 2008 samples)

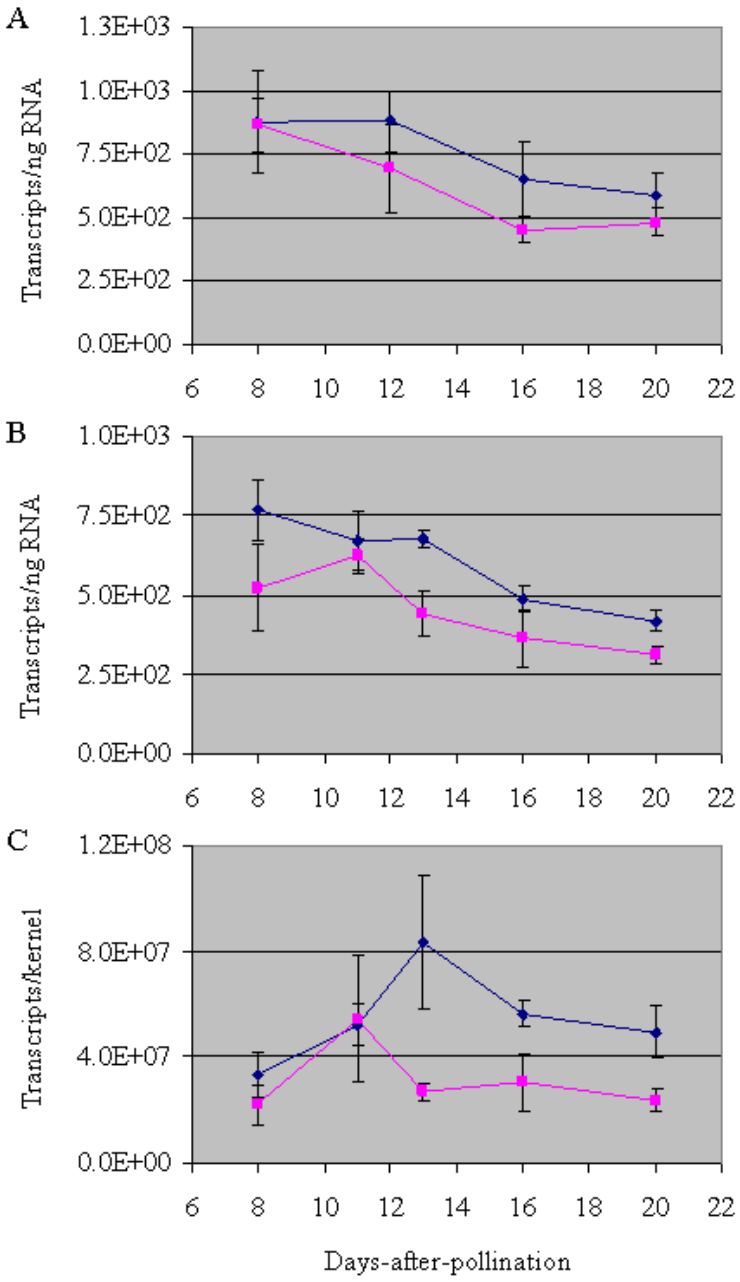

Figure 3-12. *ETR2-9* transcript levels in *Mn1* (blue) and *mn1* (pink) kernels A) transcripts per nanogram RNA (Summer 2007 samples) B) transcripts per ng RNA (Summer 2008 samples) C) transcripts per kernel (Summer 2008 samples)

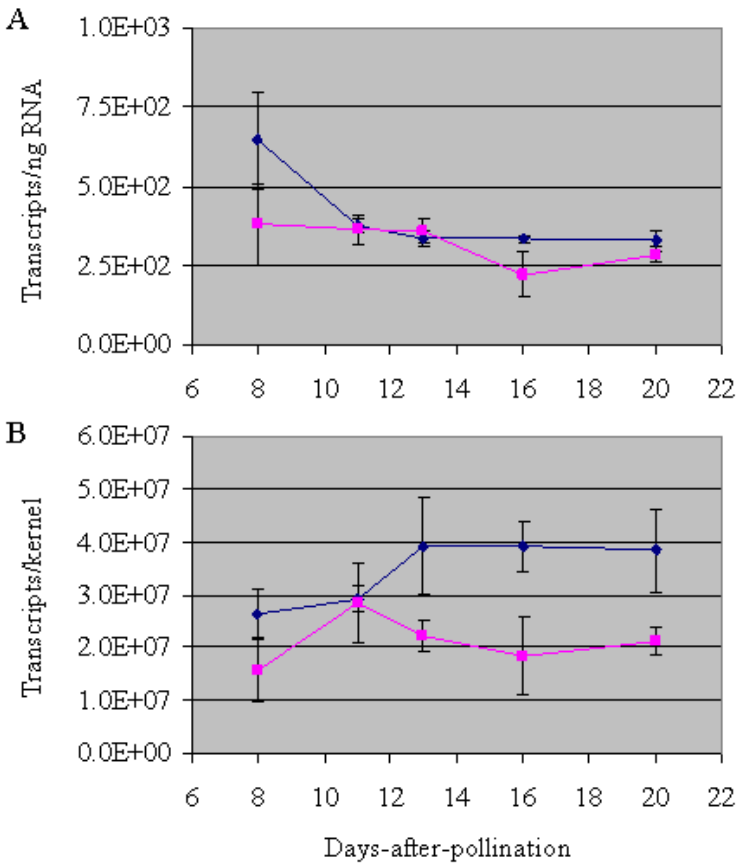

Figure 3-13. *ETR2-40* transcript levels in *Mn1* (blue) and *mn1* (pink) kernels (Summer 2008 samples) A) transcripts per nanogram RNA B) transcripts per kernel

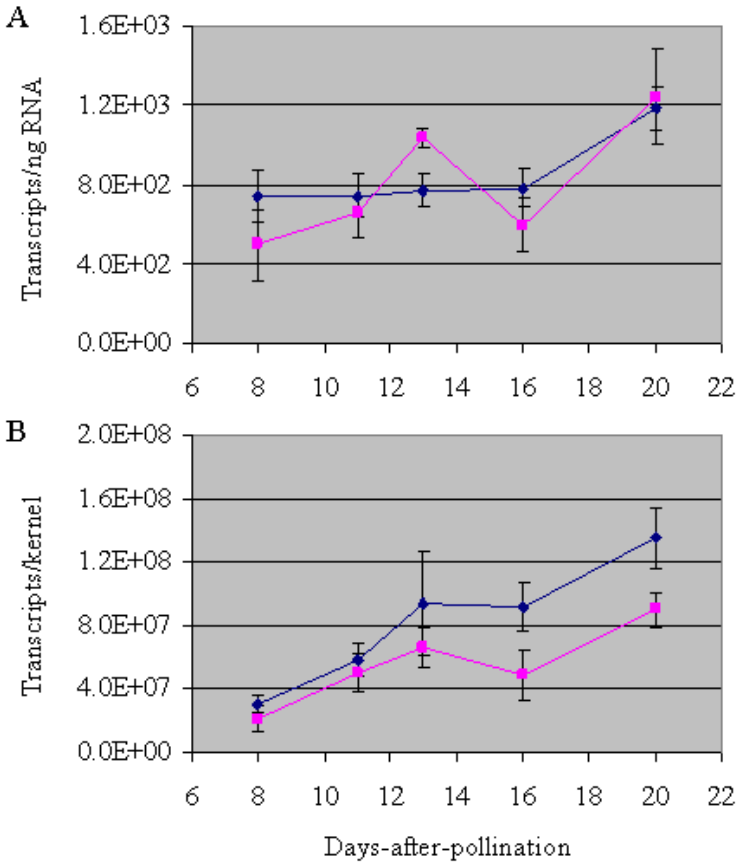

Figure 3-14. *EIL1-1* transcript levels in *Mn1* (blue) and *mn1* (pink) kernels (Summer 2008 samples) A) transcripts per nanogram RNA B) transcripts per kernel

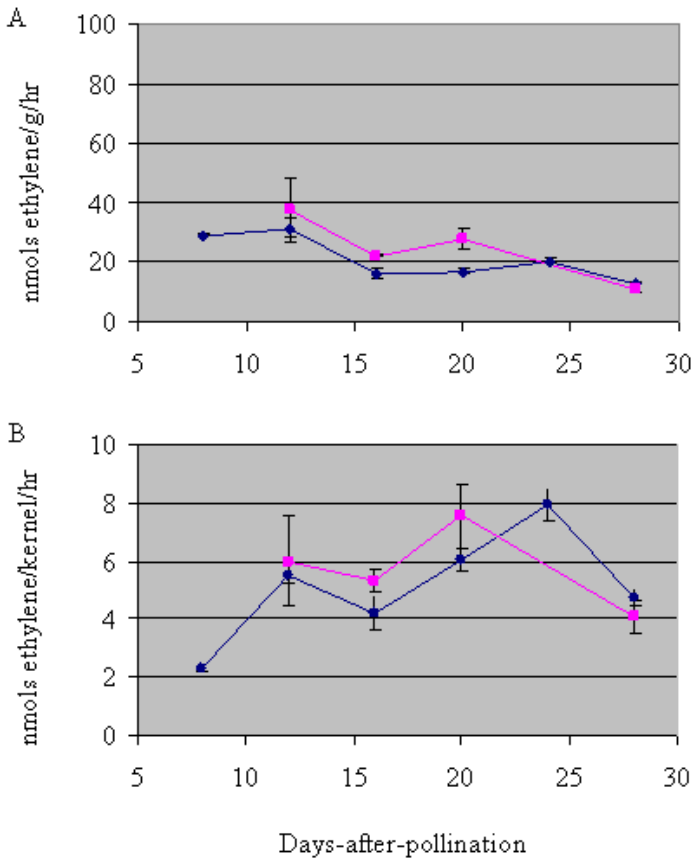

Figure 3-15. Ethylene produced by *Su1* (blue) and *su1* (pink) kernels, nmols of A) nmol/g/hour B) nmol/kernel/hour (Summer 2007 field harvest)

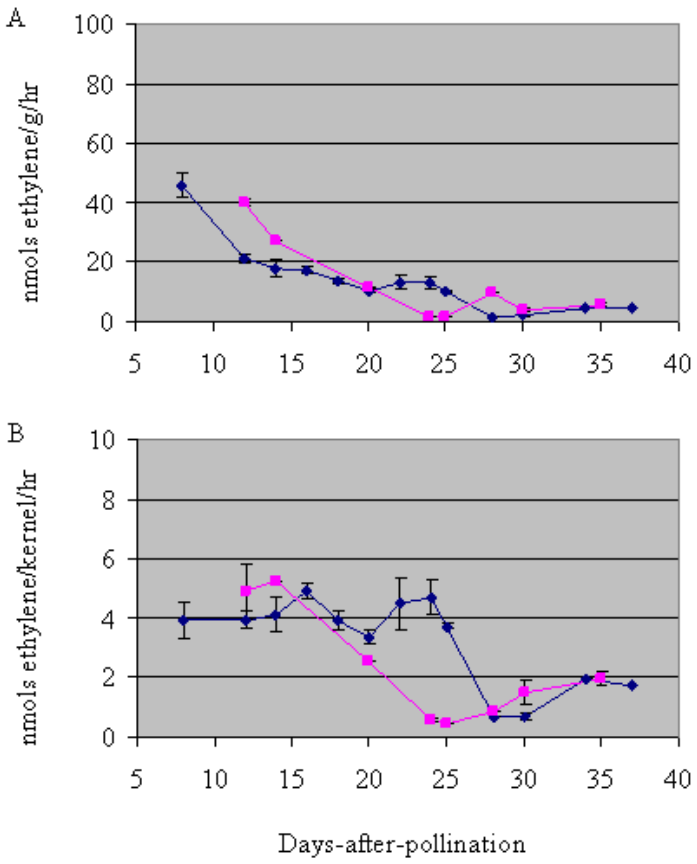

Figure 3-16. Ethylene produced by *Su1* (blue) and *su1* (pink) kernels, nmols of A) nmol/g/hour B) nmol/kernel/hour (Summer 2008 field harvest)

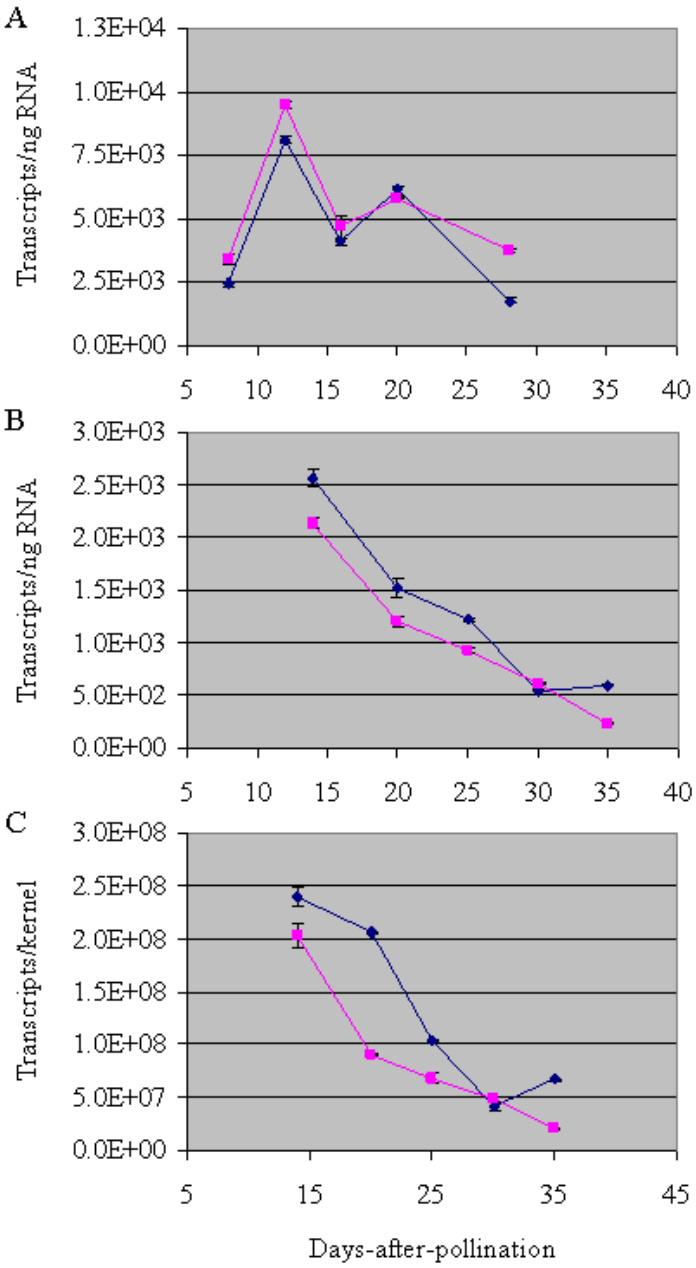

Figure 3-17. *Su1* transcript levels in *Su1* (blue) and *su1* (pink) kernels A) transcripts per nanogram RNA (Summer 2007 samples) B) transcripts per ng RNA (Summer 2008 samples) C) transcripts per kernel (Summer 2008 samples)

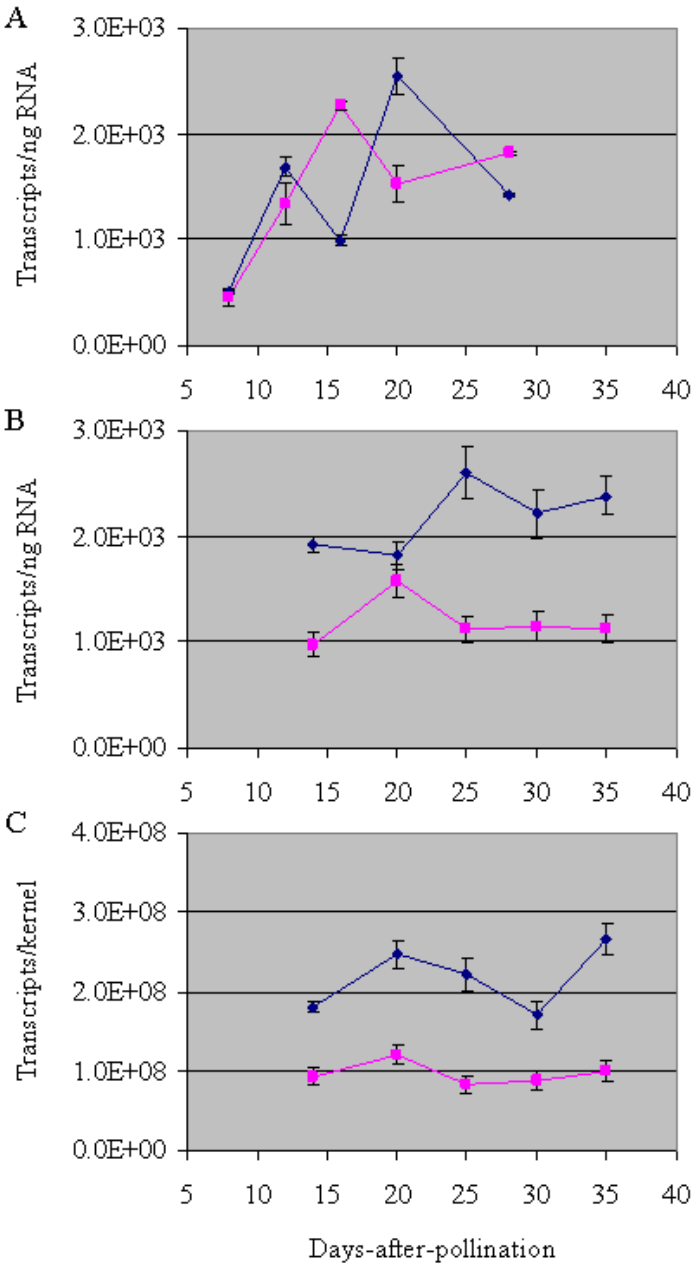

Figure 3-18. *Sus2* transcript levels in *Su1* (blue) and *su1* (pink) kernels A) transcripts per nanogram RNA (Summer 2007 samples) B) transcripts per ng RNA (Summer 2008 samples) C) transcripts per kernel (Summer 2008 samples)

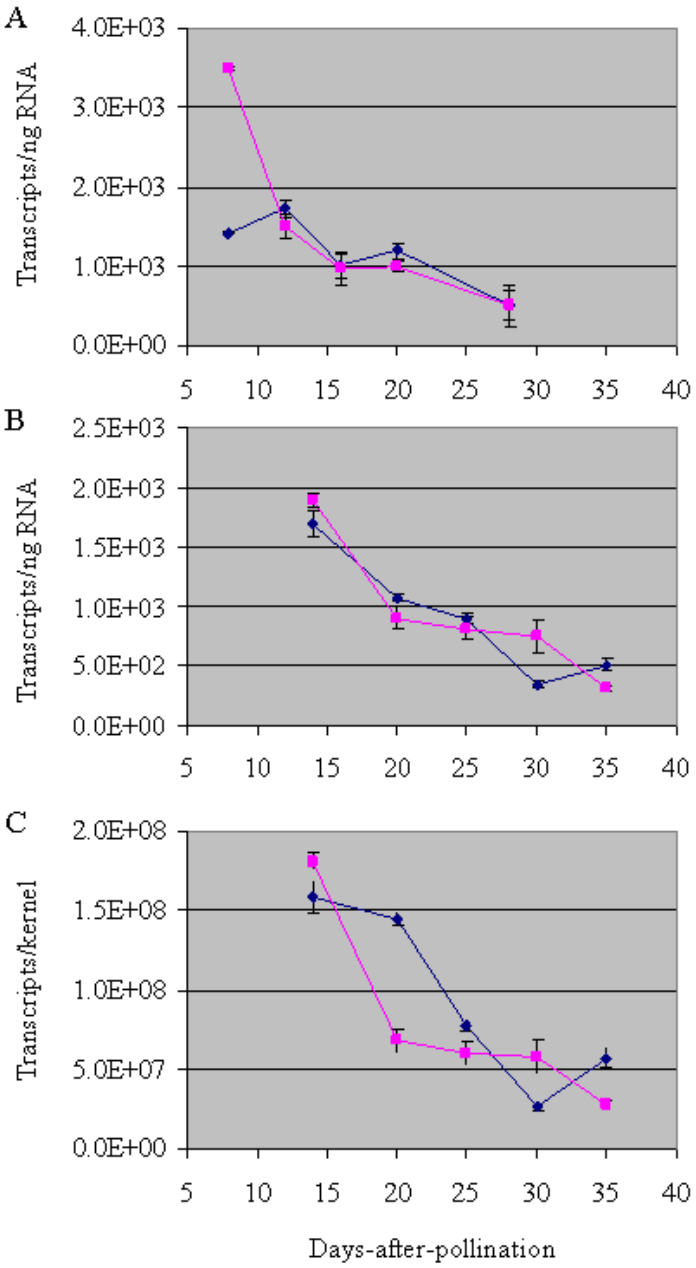

Figure 3-19. *HXK2* transcript levels in *Su1* (blue) and *su1* (pink) kernels A) transcripts per nanogram RNA (Summer 2007 samples) B) transcripts per ng RNA (Summer 2008 samples) C) transcripts per kernel (Summer 2008 samples)

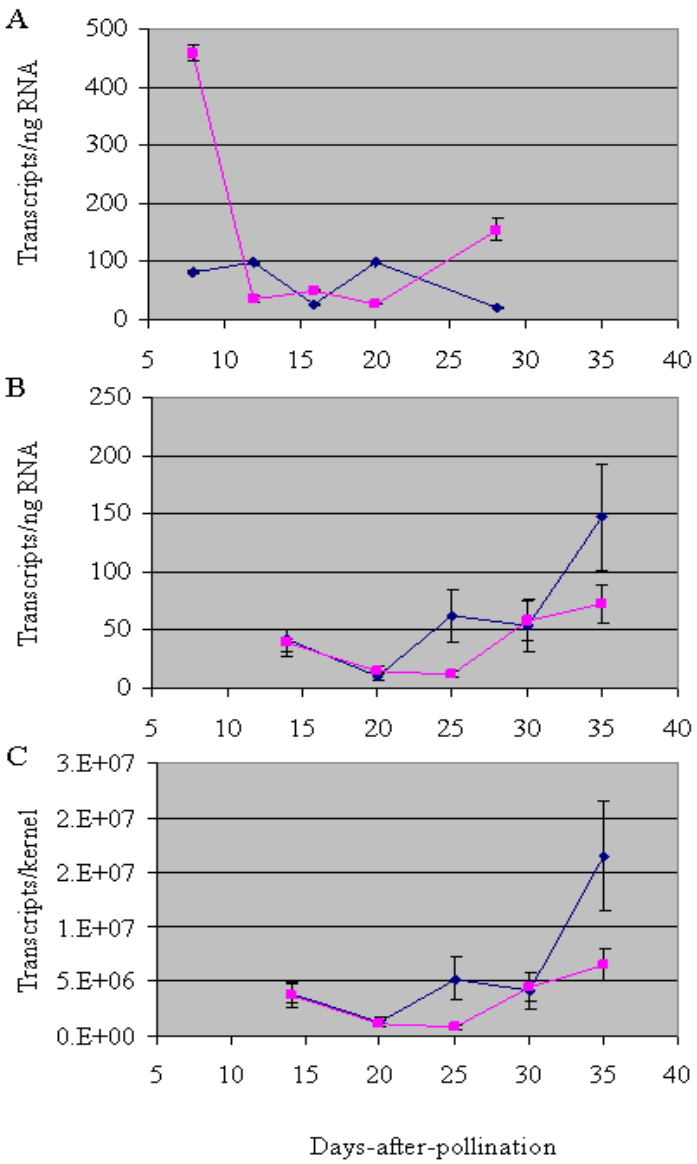

Figure 3-20. *ACS2* transcript levels in *Su1* (blue) and *su1* (pink) kernels A) transcripts per nanogram RNA (Summer 2007 samples) B) transcripts per ng RNA (Summer 2008 samples) C) transcripts per kernel (Summer 2008 samples)

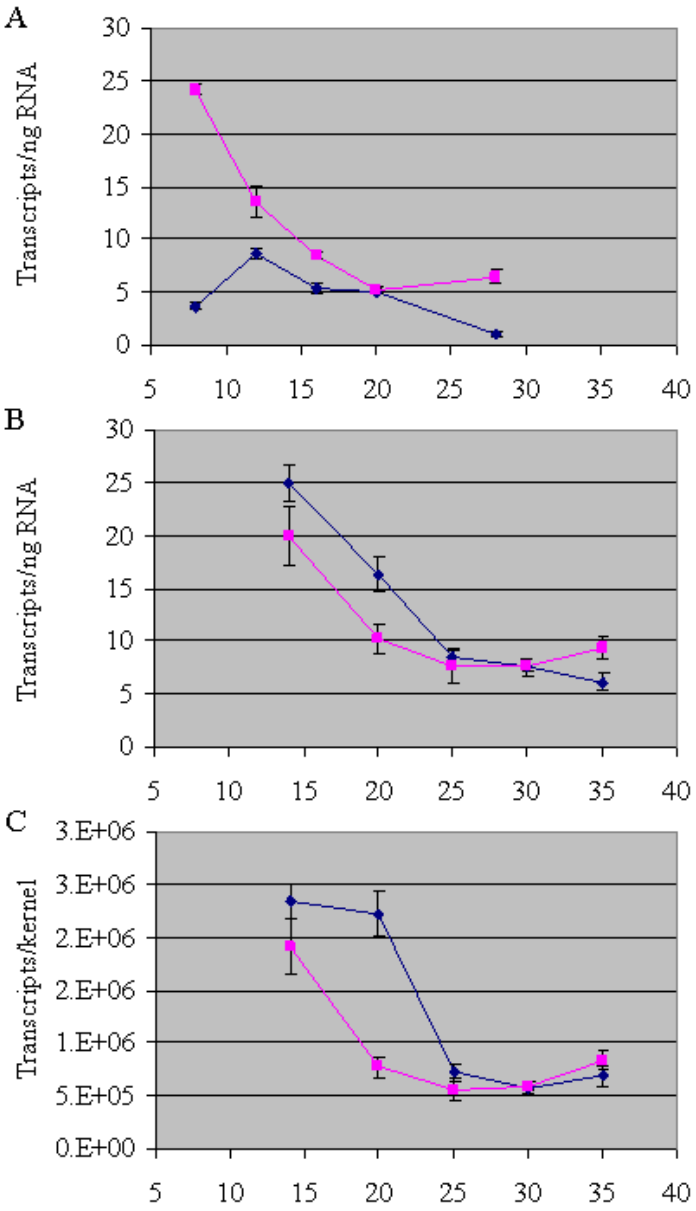

Figure 3-21. *ACS6* transcript levels in *Su1* (blue) and *su1* (pink) kernels A) transcripts per nanogram RNA (Summer 2007 samples) B) transcripts per ng RNA (Summer 2008 samples) C) transcripts per kernel (Summer 2008 samples)

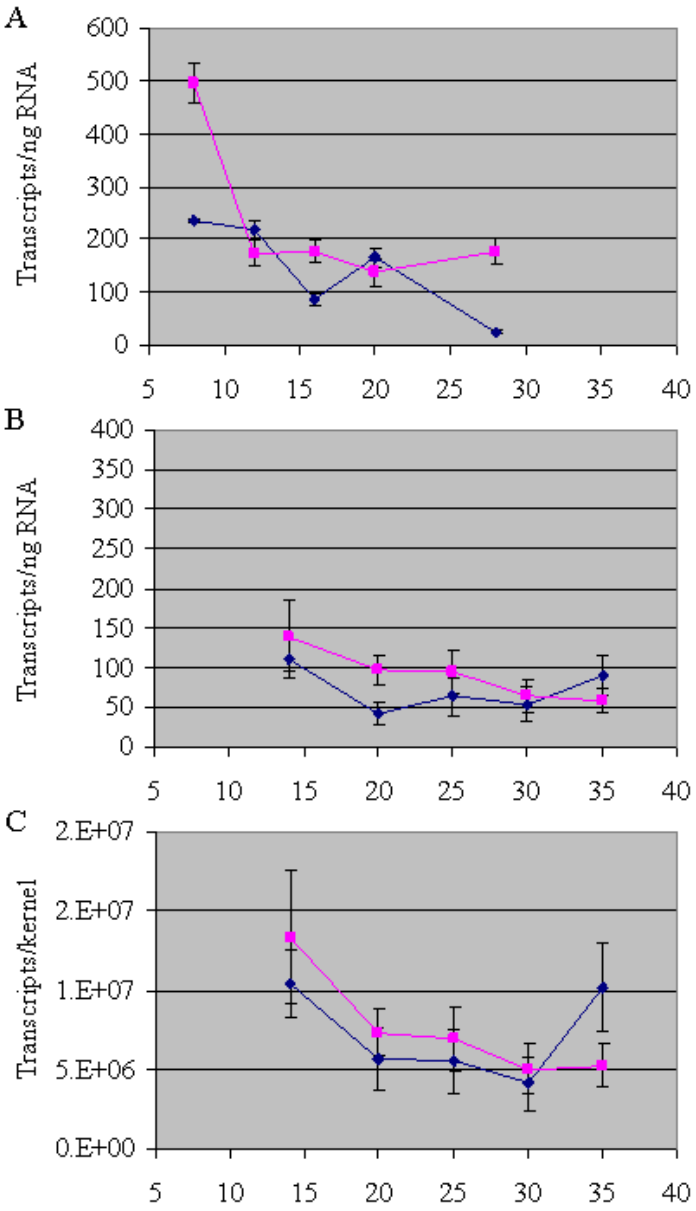

Figure 3-22. *ACS7* transcript levels in *Su1* (blue) and *su1* (pink) kernels A) transcripts per nanogram RNA (Summer 2007 samples) B) transcripts per ng RNA (Summer 2008 samples) C) transcripts per kernel (Summer 2008 samples)

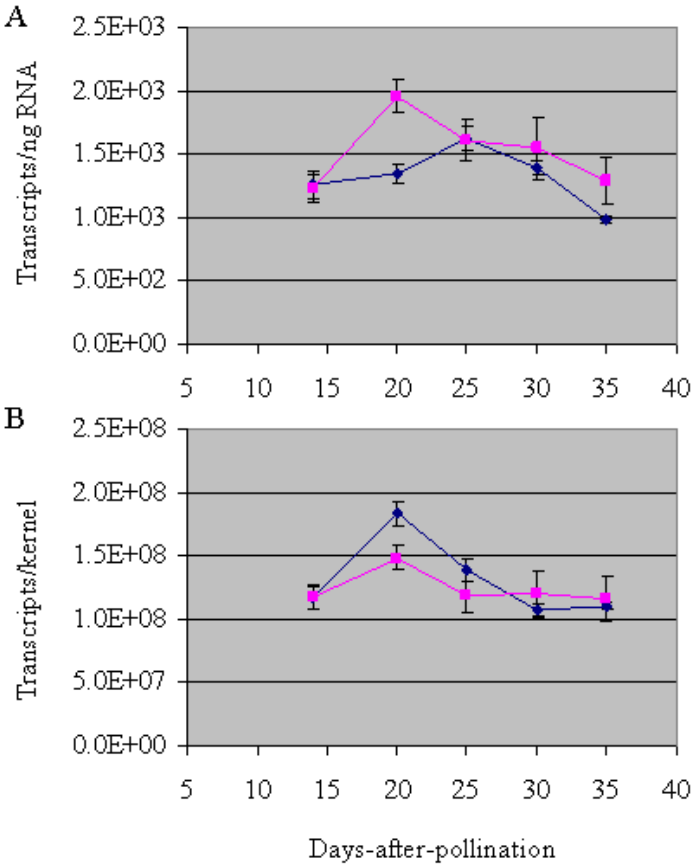

Figure 3-23. *ACO20* transcript levels in *Su1* (blue) and *su1* (pink) kernels (Summer 2008 samples) A) transcripts per nanogram RNA B) transcripts per kernel

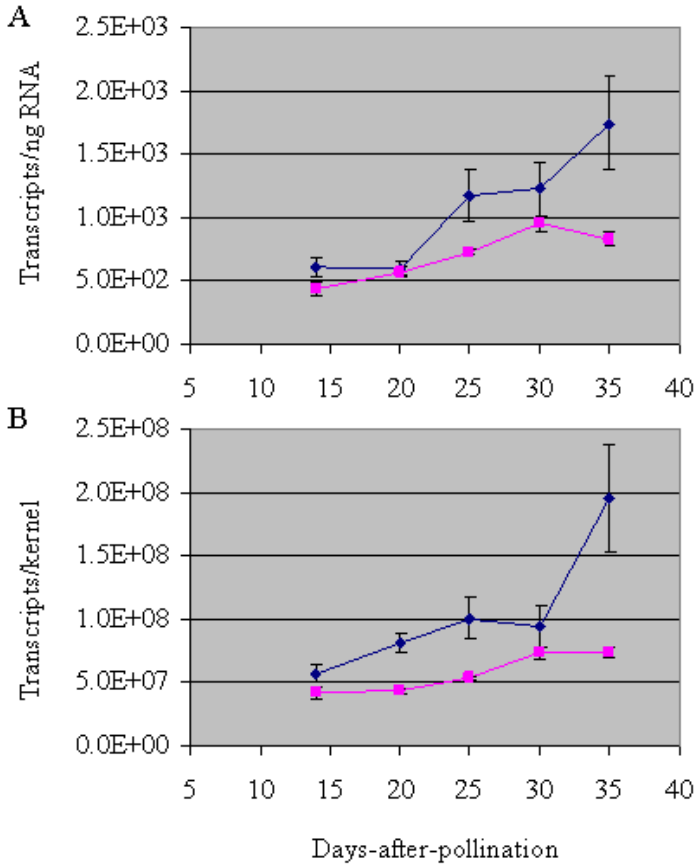

Figure 3-24. *ACO35* transcript levels in *Su1* (blue) and *su1* (pink) kernels (Summer 2008 samples) A) transcripts per nanogram RNA B) transcripts per kernel.

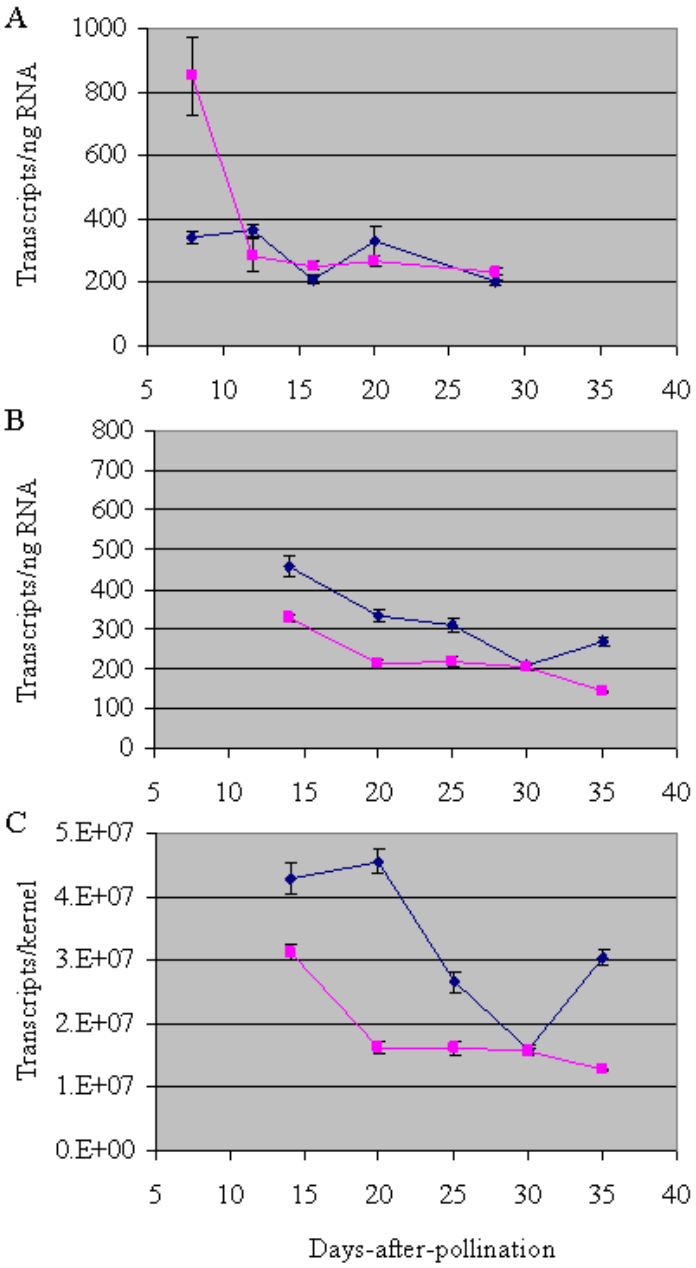

Figure 3-25. *ERS1-14* transcript levels in *Su1* (blue) and *su1* (pink) kernels A) transcripts per nanogram RNA (Summer 2007 samples) B) transcripts per ng RNA (Summer 2008 samples) C) transcripts per kernel (Summer 2008 samples)

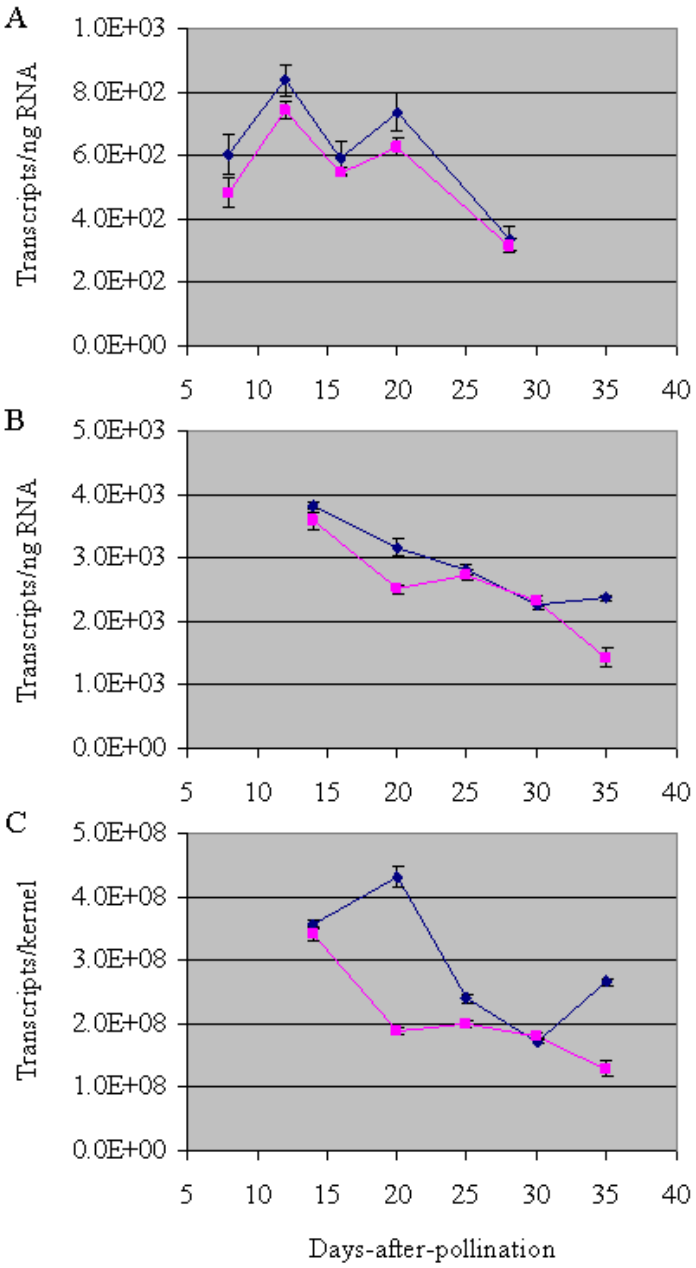

Figure 3-26. *ETR2-9* transcript levels in *Su1* (blue) and *su1* (pink) kernels A) transcripts per nanogram RNA (Summer 2007 samples) B) transcripts per ng RNA (Summer 2008 samples) C) transcripts per kernel (Summer 2008 samples)

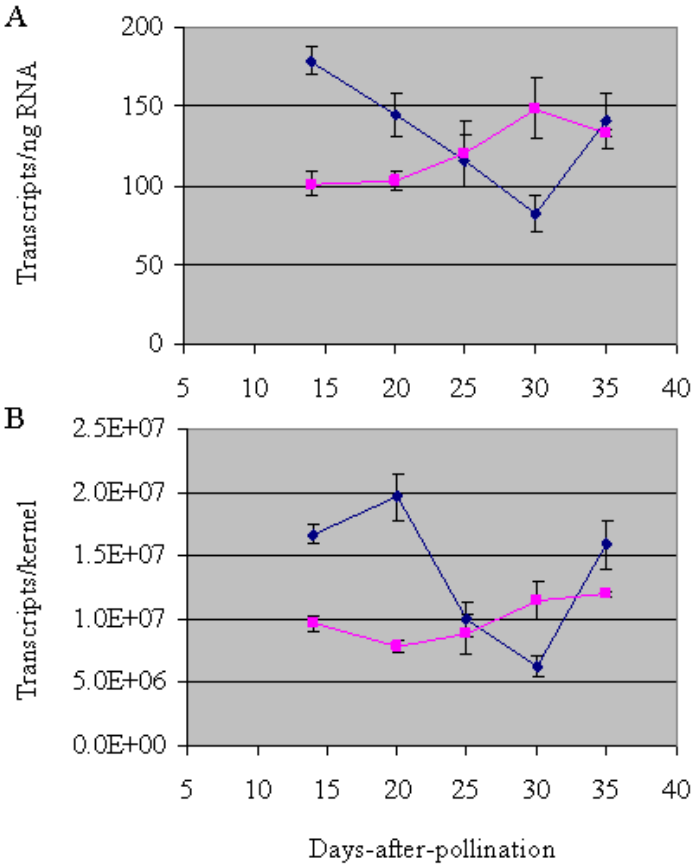

Figure 3-27. *ETR2-40* transcript levels in *Su1* (blue) and *su1* (pink) kernels (Summer 2008 samples) A) transcripts per nanogram RNA B) transcripts per kernel

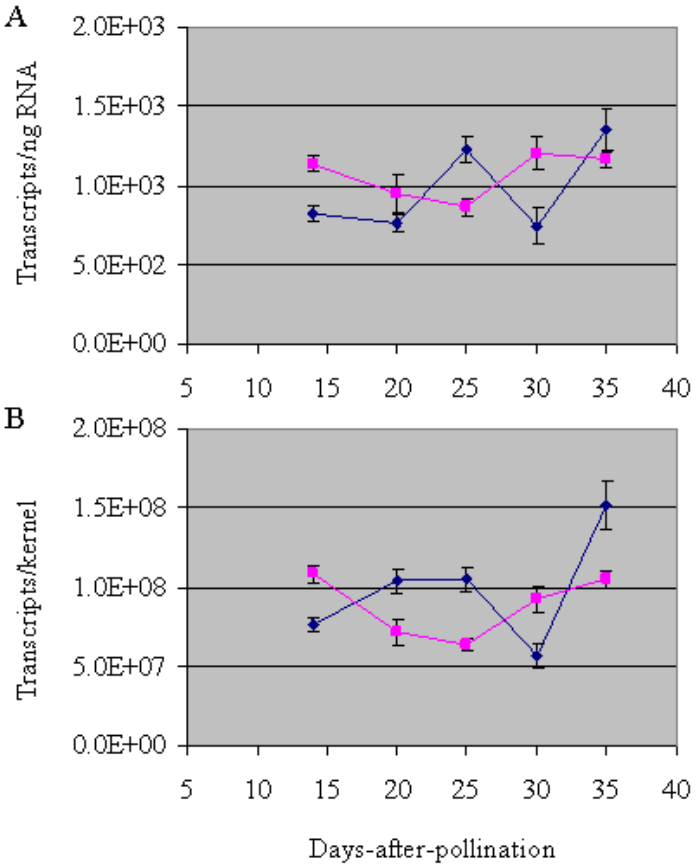

Figure 3-28. *EIL1-1* transcript levels in *Su1* (blue) and *su1* (pink) kernels (Summer 2008 samples) A) transcripts per nanogram RNA B) transcripts per kernel

CHAPTER 4
DISCUSSION

The seeds produced by *Zea mays* are important sources of energy; for human consumption, animal feed, sugar production, and recently as a source of ethanol. Given the importance of cereal crops as a whole, research dealing with seed development is valuable not only for basic science but also for many social and economic purposes. The large size of the *Zea mays* kernel makes it a good model system for cereals.

Much work has already been done to unravel the processes involved in growth and starch biosynthesis in maize seeds. Many metabolic pathways are established, from sucrose and hexose import to starch and protein synthesis (Nelson and Pan 1995; Shewry and Halford 2002; James et al. 2003). Also, the basic developmental program has been resolved, providing an outline of cell division, expansion, endoreduplication, embryo development, starch and storage protein synthesis, and finally programmed cell death of the endosperm (reviewed in Lopes and Larkins 1993; Young and Gallie 2000a). Now the most pressing questions are related to regulation and timing of these processes. Specifically, sugar and hormone interactions have emerged as critical control elements of cereal seed development. The purpose of this study is to observe the effects of two established maize kernel metabolism mutations, *mn1* and *su1*, on ethylene hormone production and related transcript levels. This should provide a basis for comparison relating sugar metabolism and hormone effects during kernel development.

The investigation of interactions between sugars and phytohormones is complicated by the fact that multiple pathways can mutually influence the processes under consideration. This phenomenon, commonly referred to as 'crosstalk,' allows slight modifications in physiology to have far-reaching consequences and effects. This also causes difficulty in determining the difference between direct and indirect interactions. Furthermore, hormone effects can be

inconsistent depending on concentrations, tissue localization, and developmental stages. For example, what holds true for germination or seedling development might be irrelevant or reversed in root meristems (Moore et al. 2003; Arteca and Arteca 2008; Gallie et al. 2009).

This report demonstrates the variable nature of ethylene production between different genetic backgrounds and developmentally altered kernel genotypes. A consistent theme is the observance of periodic bursts of ethylene production that could be related to transition through stages of kernel development.

Ethylene Accumulation in Developing Seeds

The observation of two peaks of ethylene production in developing maize kernels has been well-documented over the last 12 years (Young et al 1997; Young and Gallie 2000a; Young and Gallie 2000b). However, the specific timing, relative amplitude, and absolute levels of ethylene biosynthesis have proven variable depending on the genetic background analyzed. Young et al. (1997) suggest a partial explanation for this occurrence lies with differences in kernel mass between genotypes. In this study ethylene values were reported as a function of kernel weight and also kernel number, allowing for comparison of kernels both as biological units and as masses of tissue. In keeping with published data, discussion will focus on nmoles/kernel/hr measurements

Levels of ethylene accumulation were quantified for four genotypes during two consecutive years of field planting and harvest, generating eight individual sample series. Each of the eight series produced some form of peak of ethylene production before 20 DAP on a per kernel basis. The sizes of these peaks were between 4 and 10 nmols/kernel/hr, which is in good agreement with published values and timing (Young et al 1997; Young and Gallie 2000a; Young and Gallie 2000b).

Mn1 Seeds Produced a Distinct Peak of Ethylene between 12 and 14 DAP

Analysis of the results from *Mn1* kernels indicate that this genotype produced a peak of ethylene between 12 and 14 DAP. This is in line with the earliest recorded bursts of ethylene evolution in published reports (Young et al. 1997; Gallie and Young 2000a). Data for the *Mn1* genotype for year 2007 ethylene production paralleled the rates from the Il451b genetic background depicted in Young et al. (1997). Hormone results of the *Mn1* kernel analysis from year 2008 more closely resembled the pattern of the Oh43 results published in that same report, which generated nearly 3-fold more ethylene than the year 2007 samples before 20 DAP. This current investigation shows that, while early ethylene biosynthesis was more subtle in year 2007 samples versus the following year, the later peak at 33 DAP was more well-defined (Fig. 3-1). This is in contrast to the steady 5-7 nmol/kernel/hr of ethylene produced after 16 DAP in the year 2008 samples (Fig. 3-2B). It is possible that the 33 DAP sample from year 2007 was an anomaly since the value was derived from a single biological sample. It is also possible that sampling for year 2008 ended before a clear second developmental peak of ethylene biosynthesis could be established, given that in most previous reports, ethylene levels remained low at 32 DAP before a second peak was resolved (Young et al. 1997; Young and Gallie 2000b). Finally, differences in the technical aspects of ethylene measurement could have varied between years.

Trends in *mn1* Kernel Ethylene Production Were Varied Over Two Consecutive Years

As in the *Mn1* results, the *mn1* kernels produced a major late peak of ethylene for year 2007 samples and a dominant early peak for year 2008 samples (Figs. 3-1 and 3-2). The *mn1* genotype generated levels in the 4 nmol/kernel/hr range prior to 16 DAP during both years. However, year 2007 samples produced an apparent peak at 29 DAP more than 2-fold higher than levels at 12 DAP. As mentioned previously, the last three data points for *mn1* kernels from year 2007 were all single replicates, raising the possibility of aberrant results. Still, this pattern is in

agreement with previously published reports (Young et al. 1997), although the strongest examples of late-stage ethylene production are in high-sugar mutant lines such as *sh2*, *su1* and *su1se1*, not sugar-deficient genotypes such as *mn1*. For year 2008 samples, *mn1* seeds exhibited a maximum rate of ethylene generation at 16 DAP, roughly four days after maximal levels of INCW2 activity and ethylene peak in the wild-type kernels (Cheng et al. 1996; Fig. 3-2B). Ethylene production rates remained constant until a sharp decline at 30 DAP, as reported previously. The period from 16 to 25 DAP showed that, although ethylene production in *mn1* kernels was lower than wild-type, the smaller kernels produced nearly 2-fold higher ethylene levels on a per gram fresh weight basis. This rate was maintained throughout the period associated with initiation and progression of starch loading in wild-type kernels. Increased endogenous ethylene production as well as treatment of wild-type kernels with ethylene has been shown to accelerate cell death in developing maize seeds (Young et al. 1997; Young and Gallie 2000b).

Neither *Mn1* nor *mn1* lines showed any periods of sharp decline in ethylene levels that would clearly separate distinct peaks (Figs. 3-1 and 3-2). This relatively constant level of production is not unique when considered against previously published data, but even maize genotypes with high ethylene production rates exhibit substantial transient reductions in ethylene levels between 20 and 32 DAP (Young et al. 1997; Young and Gallie 2000b). The lack of *mn1* material in the field prevented sampling past 32 DAP; a stage that frequently involves increased hormone levels (Young et al. 1997). It is possible that 30 DAP represents the effective endpoint of *mn1* kernel development.

Hexose Deficiency and Increased Sucrose Lead to Pleiotropic Effects in Maize Seeds

While the significance of rising and falling ethylene levels as developmental cues is unknown, and sensitivity of different tissues to ethylene is another important factor, a

consistently high level of ethylene has traditionally been thought of as a stress signal promoting cell death in this tissue and stage of growth (reviewed in Young and Gallie 2000a). Auxin is shown to promote ethylene biosynthesis in various systems (Arteca and Arteca 2008). The auxin IAA, and IAA-conjugates, have been shown to increase sharply in maize kernels between 9 and 11 DAP, coinciding with reduced cytokinin (Lur and Setter 1993; LeClere et al. 2008). It is possible that the substantial rise in auxin levels 9-11 DAP contributed to the timing of the early ethylene peak in wild-type kernels. From this it follows that the auxin-deficient *mn1* line could have delayed ethylene biosynthesis at this critical stage of kernel development (LeClere et al. 2008). In addition, Li et al. (2008) report that, beginning at 12 DAP and extending through 20 DAP, *mn1* kernels exhibit increased sucrose levels versus the wild-type. Combined with data from Young et al. (1997) that demonstrated increased ethylene levels in conjunction with increased sucrose levels in *sh2* and *su1se1* mutant lines, it is possible that a relationship exists between the hexose/sucrose ratio, auxin, and ethylene levels in developing maize kernels. Previous studies of *Arabidopsis* suggest complex interactions between sugars and phytohormones, supporting the possibility of this relationship in maize kernels (Zhou et al. 1998; Cheng et al. 2002; Leon and Sheen 2003; Moore et al. 2003; Yanigisawa et al. 2003; Gibson 2004)

Su1 and *su1* Kernels Displayed Inconsistent Ethylene Production over Two Consecutive Years

According to Creech (1965) the *su1* mutation leads to 2-fold higher sucrose than wild-type by 16 DAP. At this same stage, water-soluble polysaccharides (WSP) are increased nearly 4-fold. Despite differences in sugar and starch content during early development, *Su1* and *su1* ethylene production in this report was parallel until 20 DAP (Figs. 3-15 and 3-16) and has been reported to be similar until 32 DAP (Young et al. 1997). The data presented in this report showed

a parallel relationship between *Su1* and *su1* at most stages of development (Figs. 3-15 and 3-16). However, the timing and relative amplitude between first and second ethylene peaks were dissimilar when comparing results from year 2007 and year 2008 GC analysis. This could be the result of different environmental conditions between years, leading to variations in stress factors such as drought and heat. It is possible that improved handling of samples during the year 2008 harvest increased the accuracy of the analysis. However, the range of ethylene production from year 2007 is higher than that of year 2008 for the *Su1* and *su1* kernels (Figs. 3-15 and 3-16), while the opposite is true of the *Mn1* and *mn1* samples (Figs. 3-1 and 3-2), making it difficult to attribute changes between years to systemic effects.

***Su1* and *su1* kernels showed two clear peaks of ethylene production prior to 30 DAP**

The differences between *Su1* and *su1* ethylene levels for year 2007 field samples were statistically insignificant (Fig. 3-15). Technical difficulties with the GC apparatus prevented collection of data for *su1* kernels at 28 DAP. The highest levels of hormone in *Su1* kernels were at 12 and 24 DAP, with a small decline during the intervening 12 days (Fig. 3-15B). Cumulative ethylene exposure is measured in part by ethylene receptor degradation in climacteric fruit (Kevany et al. 2007). Whether or not this paradigm holds true in maize kernels is unknown. It is important to note that the 12-DAP peak was in the 5 nmol/kernel range, and the later *Su1* peak reached 8 nmol/nL. This is in good agreement with *Mn1* and *mn1* data concerning physiologically relevant concentrations. However, the amount of ethylene required to trigger a developmental responses is unknown. In addition, ethylene perception and signaling are mediated by many factors downstream of ethylene production, and therefore inferring physiological effects based solely on hormone data is impossible (Tatsuki and Mori 2001; Yanigisawa et al. 2003; Yoo et al. 2008).

While the year 2008 data concerning *Su1* and *su1* were similar between genotypes prior to 20 DAP (Fig. 3-16), analysis revealed one major difference during development. Most importantly, the samples of *Su1* kernels from the year 2008 revealed two clear peaks, one each at 16 and 22-24 DAP, before falling 4-fold at 28-30 DAP (Fig. 3-16B). The *su1* line had a first peak of similar level two days earlier at 14 DAP (though this was a single replicate and was not enough on which to base any conclusions). However, the second peak was completely absent in the *su1* line from 20 to 25 DAP, with a 4-fold hormone reduction in the mutant kernels. This increase after a deep trough at the 25-30 DAP stage was similar to previous reports (Young et al. 1997; Young and Gallie 2000b) although the most closely-related data on *su1* from Young et al. (1997) does not show such a decline in this genotype. In that report *su1* ethylene levels rise to ~3-fold at 40 DAP over the levels in the related control genotype. Insufficient amounts of field samples prevented analysis of this later stage.

It is important to note that the most disparate levels of ethylene between the *Su1* and *su1* samples were at 24-25 DAP. These *su1* measurements were taken on July 18th and July 20th, 2008. Upon further investigation, each of the ten ears harvested on these dates generated abnormally low ethylene values. These included the *su1* samples at 24-25 DAP (Fig. 3-16), the *Su1* samples at 28 and 30 DAP (Fig. 3-16) and the *mn1* samples at 30 and 31 DAP (Fig. 3-2). It is possible that all these ages of kernels coincidently produced low amounts of ethylene at their respective stages of development, considering that published data support a transient cessation of ethylene biosynthesis (Young et al. 1997; Young and Gallie 2000b). After consulting the hard-copies of GC data from these two harvest dates, no abnormalities were apparent in either the calibration or function of the GC apparatus. The average morning temperatures for these two dates were 83.6ºF and 82.4ºF, respectively. This was similar to the temperatures on the dates that

the *Su1* ethylene peak between 22 and 25 DAP were recorded. Despite this similarity in temperature, it seems plausible that some environmental variation caused the low ethylene levels on July 18th and 20th. Because data was recorded over two different days for ten different ears, with multiple replicates per ear, experimental error is less likely.

A second peak of ethylene hormone in *Su1* samples from year 2008 showed unique timing

The occurrence of a second ethylene peak in year 2008 in *Su1* samples, just eight days after the initial peak at 16 DAP (Fig. 3-16B), was unexpected because none of the published literature reports such a quickly repeated burst of ethylene (Young et al. 1997; Gallie and Young 2000b). Each of the three data points from 22 to 25 DAP was the average of two biological replicates (Fig. 3-16B), recorded across three different dates, lending credibility to the observance of this peak. Data from Young et al. (1997) show a consistent dip in ethylene production at 24 DAP in the wild-type and three mutant lines; *su1*, *su1se1*, and *sh2*. Despite this similarity, none of those lines show such a rapid shift in hormone production. This could be partly due to the practice in all previously published work of sampling kernels at 4 DAP intervals. This methodology limits resolution of rising and falling hormone production to 8 DAP periods, possibly masking rapid bursts of ethylene generation. Still, most published ethylene data in maize kernels show sweeping curves without indication of rapid shifts. Data from various genetic backgrounds and genotypes highlight the complex nature of ethylene hormone production and measurement, and this report adds to the body of evidence supporting the sensitive nature of ethylene activity in maize kernels.

Transcript Accumulation and Correlation with Ethylene Hormone Evolution

Hormone synthesis, perception and action are regulated at many levels, with complex signals being integrated and modulated continuously. Transcript accumulation is one way to connect the involvement of a gene with certain tissues and processes. Despite the frequent

occurrence of post-transcriptional and post-translational regulation, the quantity of mRNA for a particular gene serves as a foundation for understanding the processes that affect phenotypes of biological systems.

In this study, transcript levels were analyzed for four metabolic genes and four families of genes related to ethylene biosynthesis, perception and signal transduction. Samples were collected from two consecutive years of field harvest, and transcript levels were recorded as absolute transcript levels per nanogram total RNA. The second year, additional data was recorded to allow for calculation of transcripts on a per kernel basis in order to assess the state of the kernels as biological units.

Transcript Accumulation in *Mn1* and *mn1* Genotypes

Metabolic genes

Given the centrality of the *Mn1* gene for explanation of the *mn1* phenotype, it is important to understand how *Mn1* transcript levels relate to published data on INCW2 enzyme activity. In addition, the *Mn1* transcript was used as a control in order to compare qPCR data between biological replicates. At 8 DAP, the *Mn1* transcript in the *Mn1* genotype exhibited maximum expression as a proportion of total RNA, which is consistent with maximum enzyme activity and the role of INCW2 in providing hexoses to the rapidly dividing cells between 8 and 12 DAP (Fig. 3-3A and B; Cheng et al. 1996). As cells proliferate and grow, the amount of *Mn1* transcript is down-regulated as other developmentally important genes are transcribed. On a per kernel basis, there was a temporary plateau at 13 DAP, which coincides with a period of transition from cell division to cell expansion and elongation (Kowles and Phillips 1985; Sreenivasulu et al. 2004). In the *mn1* genotype, the presence of *Mn1* transcript was less than 10% of wild-type at all stages (Fig. 3-3), though this level of transcript accumulation was well above published enzyme activity and protein levels (Cheng et al. 1996). This suggests that, while the

mn1 transcript levels were less than 10% of wild-type (Fig. 3-3), there exists one or more regulatory processes that reduced enzyme activity beyond the reduction in transcript level.

Another set of important enzymes in kernel metabolism are the sucrose synthases, which are associated with production of substrates for cell expansion as well as cell wall and starch biosynthesis (Chourey et al. 1998). Originally, *Sus2* was included in this study in order to provide an internal control for RNA quality and sample preparation efficiency due to supposed consistent expression profiles in both *Mn1* and *mn1* genotypes. The margin of error in year 2007 samples prevented any meaningful comparison of *Mn1* and *mn1* lines. Year 2008 samples showed clear differences in the timing and abundance of transcript accumulation. *Sus2* transcripts in the *Mn1* genotype increased as a portion of total RNA at 11 DAP, and on a per kernel basis at 13 DAP (Fig. 3-4). This pattern is consistent with the concept of increased *Sus2* activity promoting transition from cell division to cell enlargement around 12 DAP. Conversely, in the *mn1* line, *Sus2* had a delayed and lower abundance of transcript at 13 DAP, possibly as a result of low hexose signaling fueling developmental progress (Fig. 3-4B). On a per kernel basis, *mn1* samples displayed a brief increase of *Sus2* transcript at 11 DAP, with a subsequent decline that probably reflected the cessation of kernel expansion after ~12 DAP (Fig. 3-4C).

The *HXK2* gene showed an insignificantly higher expression in the wild-type versus the *mn1* genotype for year 2007 samples. This pattern was more clearly resolved in year 2008, when the 8 DAP stage showed 2-fold higher levels in *Mn1* kernels (Fig 3-5). This difference in expression was similar to that of the *Mn1* gene, in that levels were highest at early stages and declined steadily. The same plateau in the wild-type was seen between 11 and 13 DAP on a per kernel basis, further supporting this period as significant in developmental progression.

Overall, the hexose-related genes, *Mn1* and *HXK2*, were expressed early and declined during development in the wild-type, while *Sus2* expression rose at the 11-13 DAP transition period. Hexokinase inhibitors have been shown to impair sucrose- and hexose-dependent induction of a major sucrose synthase gene, *Sus1*, in *Arabidopsis* leaves, and specific forms of the sucrose synthase enzyme family are reported to be individually regulated by sugar status (Koch et al. 1992; Ciereszko and Kleczkowski 2002). The published data provide insight into possible causes of delayed and reduced *Sus2* expression in *mn1* seeds as a result of low hexose/sucrose ratio. These changes in INCW2-deficient kernels highlight the pleiotropic effects of the *mn1* seed mutation and resulting hexose deficiency during a critical stage of early kernel development.

Ethylene biosynthesis genes of the *ACS* and *ACO* families

As actuators of the rate-limiting step in ethylene biosynthesis, ACC synthase enzymes are important targets for regulation of hormone effects. Levels for all three of the *ACS* genes currently identified in maize were an order of magnitude higher than published results, expressed both as a function of total RNA and as whole kernel data (Figs. 3-6 to 3-8; Gallie and Young 2004). This could be partially due to differences in genetic background used in the two studies. Additionally, the soil composition, temperature, water supply and light characteristics of the environment were possible factors in physiological variation. However, the relative contributions of each *ACS* gene to total *ACS* transcript levels were in agreement with Gallie and Young (2004): *ACS2* was most abundant, followed by *ACS7,* and *ACS6* was the least-expressed.

Few significant differences were seen between *Mn1* and *mn1* samples for the *ACS* family (Figs. 3-6 to 3-8). The *ACS2* and *ACS6* transcripts were more abundant in wild-type than *mn1* at 8 DAP, but large standard error prevented solid conclusions. All three family members displayed a constant or slightly downward trend in both genotypes, on a per ng total RNA and per kernel

basis. This trend was not dissimilar to the wild-type results of Gallie and Young (2004), given that data in the current study covered only early development for *Mn1* and *mn1*. The most compelling observation was from *ACS6* data, which showed a clear increase in transcript levels at 13 DAP in the wild-type from year 2008 (Fig 3-7B and C). The transcript levels at this stage coincided with the peak in ethylene evolution in the same samples (Fig 3-2B) and also matched the timing of *ACS6* transcript in Gallie and Young (2004).

A disproportionate contribution of the three *ACS* genes to ethylene biosynthesis is demonstrated in maize leaf tissue (Young and Gallie 2004).The loss of *acs2* function reduces ethylene levels by 50%, compared with a mutation in the *acs6* gene that causes a 90% reduction in hormone levels. Even though the ACS proteins are subject to extensive post-transcriptional regulation (Tatsuki and Mori 2001; Liu and Zhang 2004; Sebastia et al. 2004), the data presented in Figures 3-6 through 3-8 are in agreement with the disproportionate contribution of *ACS6* transcript levels to increased ethylene biosynthesis described previously (Young and Gallie 2004). This observation is based primarily on the correlation of *ACS6* transcript with ethylene evolution in 13 DAP *Mn1* kernels (Fig. 3-7).

The ACC oxidase family is comprised of four members in maize, three of which are expressed in kernels (Gallie and Young 2004). These enzymes convert ACC produced by ACC synthase into ethylene, which is then free to diffuse through tissues and interact with receptors. Two genes of the ACC oxidase family were analyzed in year 2008 samples only. The highly-similar *ACO20* and *ACO35* genes showed relative expression rates similar to those published by Gallie and Young (2004), although absolute abundance shown here was again an order of magnitude higher than their published work. The peak levels in *ACO35* transcripts, shown here at 13 DAP, were similar in both *Mn1* and *mn1* genotypes (Fig 3-10B) and were in agreement

with data published in Gallie and Young (2004). Compared to the wild-type, a higher proportion of *ACO20* transcript was found in *mn1* kernels at 13 and 20 DAP based on # transcripts/ng total RNA (Fig. 3-9). There is no reason to conclude that this is related to higher ethylene synthesis in the *mn1* line from 16 DAP onward, although the difference at 13 DAP could be indicative of increased induction of ethylene-related transcripts at the expense of normal storage gene synthesis. *ACO20* transcript levels in wild-type kernels maintained constant expression per ng total RNA during development, which supports the observation of Gallie and Young (2004) that this gene is not induced early in endosperm growth.

Ethylene receptor genes and *EIL1-1*

Ethylene receptors are critical components of ethylene signaling. They function as negative regulators of ethylene response that are inactivated upon binding of the ethylene molecule (Hua and Meyerowitz 1998). All four of the known maize ethylene receptors are expressed in maize kernels (Gallie and Young 2004). The three receptor transcripts examined here, *ERS1-14*, *ETR2-9* and *ETR2-40*, followed a general pattern of decline from 8 to 20 DAP in terms of relative mRNA abundance (Figs. 3-11 to 3-13), with the *ETR* transcripts slightly more numerous than *ERS1-14*. Both of these observations are in agreement with results published by Gallie and Young (2004).

For the *ERS114* transcript, little difference between the *Mn1* and *mn1* genotypes was apparent in year 2007 samples (Fig. 3-11A). Data from year 2008 showed a distinct and consistent difference between *Mn1* and *mn1* kernels at 11 DAP (Figure 3-11B). This is another example of a variation in the *mn1* samples that coincides with a critical period in kernel development and transcriptional reprogramming. While increased *ERS1-14* transcript in itself does not reveal the status of the ERS1-14 protein, and the direct cause of transcriptional

modulation for this gene is unknown, correlative evidence connects a transient increase in *ERS1-14* levels to decreased glucose and/or auxin levels as a result of the *mn1* mutation.

The two *ETR2* genes showed similar expression between *Mn1* and *mn1* genotypes at 8 and 11 DAP on a per kernel basis. While the *Mn1* samples showed an increase in *ETR2* transcript at 13 DAP, the *mn1* samples transcript levels decreased, and both lines remained level during subsequent development (Figs. 3-12C and 3-13C). This could be explained by differences in kernel size. *Mn1* and *mn1* kernels have similar characteristics until 11 DAP, at which point the *miniature* phenotype leads to impaired growth in the hexose-deficient mutant seeds. This trend of transcript reduction in *mn1* kernels was visible in the *ERS1-14* results as well, but differences were not statistically significant. Overall it seems that the *mn1* mutation did not affect transcription of *ETR2* ethylene receptor genes in developing maize seeds, and only impacted *ERS1-14* transcript levels during the 11-13 DAP transition period.

Gallie and Young (2004) note similarities between the pattern of receptor expression and the downstream signaling components *EIN2*, *EIL1-1* and *EIL1-3*. While only *EIL1-1* transcript data is reported here, the trend was similar to that of the receptor genes. At all stages the trends of *EIL1-1* transcript levels were similar between *Mn1* and *mn1* lines, with a notable reduction visible in *mn1* kernels at 13 DAP that correlated with reduction in kernel size relative to wild-type (Fig. 3-14). *EIL1-1* transcripts increased from 8 to 20 DAP in both lines, possibly facilitating increased ethylene signaling as kernels mature. These data do not support a possibility for transcriptional modulation of *EIL1-1* due to the *mn1* mutation.

Transcript Accumulation in *Su1* and *su1* Genotypes

Metabolic genes

Due to difficulty producing an adequate supply of field-grown samples, the transcript levels for *Su1* and *su1* genotypes were the results of single biological sample analysis at each

time point. Dinges et al. (2001) report that the reference *su1* mutation reduces SU1 protein accumulation while leaving transcript levels unchanged. The use of the *Su1* transcript as an internal control is of critical importance because of the expected similarity in *Su1* transcript levels between the mutant and wild-type kernels. However, the published data focuses on a single time point (20 DAP) and the use of RNA gel blot analysis to quantify transcript levels (Dinges et al. 2001). With that in mind, both year 2007 and year 2008 results showed similar levels of *Su1* and *su1* transcript as a proportion of total RNA for all stages (Fig. 3-17 and 3-18 A and B), lending credibility to the accuracy of the assay. The observation that *su1* kernels exhibited fewer *Su1* transcripts per kernel at 20 DAP could be a result of chance selection of smaller kernels for that time point. Additionally, *su1* kernels could have had higher water content but reduced dry weight during this stage, leading to an overall lower production of RNA per kernel. When the singular nature of the 20 DAP *su1* sample is considered, a lower efficiency of RNA isolation would also have led to an inaccurate determination of total RNA per kernel, thus skewing transcript results. Also, transcriptional control of *Su1* is poorly understood, and could be related to the drastically altered sugar and starch profile present in the *su1* genotype (Creech 1965; Dinges et al. 2001).

The hexokinase *HXK2* transcript levels paralleled the trend of *Su1* transcript results (Fig. 3-17 and 3-19). *HXK2* showed similar trends of transcript expression between *Su1* and *su1* genotypes (Fig. 3-19). Highest levels of transcript accumulation were during times of peak cell division during early development. There was no apparent transcriptional modulation of *HXK2* as a result of the *su1* mutation.

While *Su1* and *HXK2* transcript levels were similar between wild-type and *su1* kernels, the levels of *Sus2* showed different responses based on genotype in the single replicates shown here

(Fig. 3-18). The most consistent response was in year 2008 samples, where *Su1* samples produced more *Sus2* transcript than the *su1* mutant at all stages except 20 DAP (Fig 3-18B and C). Higher sucrose levels in the *su1* genotype could be one explanation for lower *Sus2* expression. It is important to note that in this study, both the *mn1* and *su1* genotypes caused higher levels of sucrose relative to the wild-type kernels, and there were decreased levels of *Sus2* transcript that correlated with that modification of sugar status. Because the correlation between *Sus2* transcript levels and SUS2 enzyme activity is unknown, further analysis is needed to understand the function of *Sus2* in this system.

Ethylene biosynthesis genes of the *ACS* and *ACO* families

The ACC synthase family showed largely unrelated patterns of expression over two consecutive years. For year 2007 samples, all three *ACS* genes were strongly expressed in *su1* kernels at 8 and 28 DAP versus wild-type (Figs. 3-20A to 3-22A). The period from 12 to 20 DAP was more similar between lines, to the point that no significant difference was apparent. Why the earliest and latest stages would show such variation is perplexing, considering that ethylene production was similar at all stages (even though the 8 DAP *su1* sample was unavailable for ethylene analysis). The lack of replication leads to the conclusion that experimental error and random variation are as likely as any biological explanation for the differences at 8 and 28 DAP. One consistency is that *ACS7* and *ACS2* mRNAs were more abundant than *ACS6*, in agreement with other data presented in this report (Figs. 3-20A to 3-22A).

Concerning year 2008 samples, the relative contributions of each family member to total transcript amounts were in agreement with year 2007 data, in that the *ACS2* and *ACS7* transcripts showed up to 10-fold higher expression than *ACS6* (Figs 3-20 to 3-22). For *ACS2*, expression was identical between *Su1* and *su1* samples at 15 and 20 DAP (Fig. 3-20 B and C), which is a

period marked by higher sucrose in the *su1* line. It is logical to hypothesize that an effect due to sugar status would manifest itself during this stage, but this was not reflected in the data. At 25 DAP both *ACS2* transcript and ethylene levels were elevated in the *Su1* genotype. At the same time point *ACS2* transcript and ethylene levels were low in the *su1* mutant (Figs. 3-15 and 3-20). This suggests a possible correlation between this ACC synthase isoform and ethylene production at this stage in development. Overall levels of *ACS2* transcript rose throughout development in both genotypes, further supporting *ACS2* as a developmentally-modulated gene.

The *ACS7* transcript, when translated, shares 95% amino acid identity with translated *ACS2* (Gallie and Young 2004). However, *ACS7* showed a different pattern of expression than the highly-similar family member. There was a slight decline in *ACS7* transcript levels during development. Overall there was no significant difference in *ACS7* transcript abundance between *Su1* and *su1* kernels (Fig. 3-22B and C). While the contribution of the *ACS7* gene product to ethylene levels in maize kernels cannot be deduced from transcript data alone, the observation of relatively constitutive expression does not support the possibility of transcriptional regulation due to developmental or metabolic cues.

The levels of *ACS6* transcript were similar between wild-type and *su1* samples at all stages except 20 DAP (Fig. 3-21B and C). In contrast to the other family members, *ACS6* was maximally expressed at the earliest stage tested. This is in agreement with transcript levels published in Gallie and Young (2004) and supports the possibility that *ACS6* is specifically involved in early ethylene biosynthesis, and is in part specifically up-regulated at this stage.

Ultimately, few conclusions can be drawn from such preliminary data concerning transcriptional regulation of the ACC synthase family in developing maize kernels. *ACS6* appeared to be more highly expressed during early stages, while *ACS2* was more prominent later

in development. *ACS7* transcript showed little variation during the period of development investigated here. These observations are in general agreement with results from Gallie and Young (2004a), but further analysis is required for validation.

Transcripts for the ACC oxidase genes *ACO20* and *ACO35* were present at all stages of development tested. *ACO20* was again the more highly expressed of the two family members (Figs 3-23 and 3-24). The *Su1* and *su1* genotypes were similar with respect to *ACO20* accumulation; with relatively constant expression from 15 to 35 DAP. The *ACO35* transcript levels in both genotypes showed a modest increase as kernels developed (Fig. 3-24), possibly providing ACO enzymes in order to increase ethylene evolution during maturation. Results for the two *ACO* members investigated here showed similarity between *Su1* and *su1* genotypes. However, *ACO35* transcript levels were highest at early stages in the report by Gallie and Young (2004), contrary to data presented in this report. One possibility is that isoforms of the *ACO* family could be differently regulated as a result of changes in genetic background. With only single biological samples to draw data from, it is beyond the scope of this study to make such a claim. Similarities between *Su1* and the mutant genotype lead to the conclusion that transcriptional modulation of the *ACO* genes as a result of the *su1* mutation was unlikely during the stages tested.

Ethylene receptor genes and *EIL1-1*

The *ETR2-9* and *ERS1-14* transcripts quantified in *Su1* and *su1* samples from year 2007 showed dissimilar patterns of expression (Figs 3-25A and 3-26A). The *ETR2-9* transcript was most abundant and coincided with ethylene levels (Fig. 3-15). *ERS1-14* had a constant level of expression except for a substantial increase in 8 DAP *su1* kernels (Fig. 3-25A). This singular variation was not repeated in any other receptor data, casting doubt on the accuracy of this result

and emphasizing the need for biological replication. There was no significant difference between *Su1* and *su1* genotypes for either receptor other than the anomalous 8 DAP *ERS1-14* time point.

For year 2008 samples, both *ERS1-14* and *ETR2-9* had similar trends and quantities of expression in both wild-type and *su1* kernels (Figs 3-25 and 3-26). The *ETR2-40* results showed more variation between genotypes, with a higher amount of transcript in the *Su1* line at the earliest stage (Fig. 3-27). The most significant difference was the higher receptor transcript levels in *Su1* versus *su1* at 35 DAP. This is the time when *su1* kernels begin to produce substantially more ethylene than wild-type (Young et al. 1997), which would be exacerbated by lower receptor levels leading to increased sensitivity. The observation that receptor levels began to rise as ethylene increased in the *Su1* genotype raised the possibility that ethylene activity increased transcription of the receptors. However, no changes in ethylene levels were observed in these samples, contrary to published data (Young et al. 2007) Also, receptor transcript levels do not always correlate with protein accumulation (Kevany et al. 2007). It is possible that ethylene action simultaneously induces receptor transcript and prevents receptor protein accumulation depending on the activity of tissue-specific control mechanisms, as seen in transcript and protein levels of ripening tomato fruits (Kevany et al. 2007).

The *EIL1-1* transcript level increased modestly during development, with similar expression in *Su1* and *su1* samples (Fig. 3-28). An increase in the *EIL1-1* transcript, if it led to increased protein accumulation and activity, could facilitate increased ethylene signaling during the later developmental stage associated with kernel maturation. However, since quantitative protein data is unavailable, further work is needed to connect transcript levels with ethylene responses. No transcriptional differences between wild-type and *su1* genotypes were clear from the data shown.

CHAPTER 5
CONCLUSIONS

This report has demonstrated that patterns of biosynthesis of the phytohormone ethylene were affected by the *mn1* mutation in developing maize seeds. In addition, data presented here documented variance in hormone levels based on the genetic background of wild-type and mutant genotypes. The *mn1* mutation led to an increase in ethylene production rates in the smaller kernels during the 16-25 DAP stage, adding to the list of pleiotropic effects attributed to loss of INCW2 enzyme activity. Variance based on genetic background was highlighted by the novel results of *Su1* kernel analysis, which showed a second burst of ethylene production at 24 DAP, shortly after the initial peak at 16 DAP. This pattern is unique when compared to the results of *Mn1* and *mn1* kernels analyzed during the same period, as well as previously published reports.

Transcript levels of several genes were shown to be affected by the *mn1* mutation. For the first time, to the author's knowledge, the *Mn1* transcript was quantified in developing seeds and shown to be present in the *mn1* mutant kernels at levels between 5 and 10% of the related wild-type samples. Both *Sus2* and *HXK2* transcripts were reduced in the hexose-deficient *mn1* genotype. Of the three ACC synthase genes, transcript levels of *ACS6* appeared to be the most closely-correlated to rates of ethylene production. This is in agreement with previous reports on the importance of this gene in ethylene biosynthesis in other tissues. The levels of *ACS7* transcripts were largely constant throughout development in all genotypes tested, leading to the possibility that this ACC synthase transcript was not regulated via developmental cues. Transcript levels of the ACC oxidase genes were similar in *mn1* kernels compared to the wild-type control. However, a slightly higher level of transcript was evident in the mutant genotype at 13 DAP for both *ACO20* and *ACO35*. The difference in *ERS1-14* transcript level, which was

increased in the *mn1* samples over the levels in *Mn1* kernels, was only observed at the 11-13 DAP period associated with transition from cell division to cell expansion. Transcript data for the *ETR2* receptors were similar in both *Mn1* and *mn1* genotypes. The *EIL1-1* transcript was more abundant as development progressed in both genotypes in what appeared to be a developmentally-regulated process.

Transcript levels for isoforms of the ACC synthase, ACC oxidase and ethylene receptor gene families showed some developmental regulation between family members, but little transcriptional variation was clearly attributable to the *mn1* mutation.

Due to the lack of biological replication, conclusions based on transcript data from *Su1* and *su1* genotypes are tenuous. The *HXK2* transcript levels appeared unchanged, while the *Sus2* levels were clearly modified in the high-sucrose *su1* kernels. Transcripts of the ACC synthase genes *ACS2* and *ACS7* were much more abundant than those of *ACS6*, in agreement with data from *Mn1* and *mn1* kernels. A higher proportion of *ACS6* transcript was present during early stages, while *ACS2* transcripts were more abundant during later development. *ACS7* transcript levels appeared to be constitutive in both genotypes throughout kernel growth. The ACC oxidase transcripts were similarly expressed in both *su1* and the wild-type kernels, with *ACO35* increased during later stages of growth. The ethylene receptor expression in both *Su1* and *su1* genotypes decreased during development, with little difference in transcription between wild-type and mutant kernels. Conversely, *EIL1-1* transcript levels rose in both genotypes over time, consistent with a role in ethylene signaling during PCD and kernel maturation during late development.

In summary, the biosynthesis of ethylene in developing maize kernels is a complex result of many interacting factors, one of which is sugar status in developing seeds. Correlations between hormone levels and transcript levels of sugar- and ethylene-related genes provide a

basis for further investigation of the process involved in maize kernel development. Both the similarities and differences between wild-type and mutant maize genotypes offer additional insight into the genetic interactions influencing kernel development.

LIST OF REFERENCES

Alonso JM, Hirayama T, Roman G, Nourizadeh S, Ecker JR (1999) EIN2, a bifunctional transducer of ethylene and stress responses in *Arabidopsis*. Science 284:2148-2152

Beatty MK, Rahman A, Cao H, Woodman W, Lee M, Myers AM, James MG (1999) Purification and molecular genetic characterization of ZPU1, a pullulanase-type starch Debranching enzyme from maize. Plant Physiol 119:225-266

Beckles DM, Smith AM, Rees T (2001) A cytosolic ADP-glucose pyrophosphorylase is a feature of graminaceous endosperms, but not of other starch-storing organs. Plant Physiol 125:818-827

Bhave MR, Lawrence S, Barton C, Hannah LC (1990) Identification and molecular characterization of *Shrunken-2* cDNA clones of maize. Plant Cell 2:581-588

Black RC, Loerch JD, McArdle FJ, Creech RG (1966) Genetic interactions affecting maize phytoglycogen and the pyytoglycogen-forming branching enzyme. Genetics 53:661-668

Bosnes M, Weideman F, Olsen OA (1992) Endosperm differentiation in barley wild-type and sex-mutants. Plant J 2:661–674

Boyer CD, Preiss J (1978) Multiple forms of starch branching enzyme of maize: evidence for independent genetic control. Biochem Biophys Res Comm 80:169-175

Cao H, Imparl-Radosevich J, Guan H, Keeling PL, James MG, Myers AM (1999) Identification of the soluble starch synthase activities of maize endosperm. Plant Physiol 120:205-215

Chao Q, Rothenberg M, Solano R, Roman G, Terzaghi W, Ecker JR (1997) Activation of the ethylene gas response pathway in Arabidopsis by the nuclear protein ETHYLENE-INSENSITIVE3 and related proteins. Cell 89:1133–44

Cheng WH, Tallercio EW, Chourey PS (1996) The *Miniature1* seed locus of maize encodes a cell wall invertase required for normal development of endosperm and maternal cells in the pedicel. Plant Cell 8:971-983

Cho YH, Yoo SD, Sheen J (2006) Regulatory functions of nuclear Hexokinase1 complex in glucose signaling. Cell 127:579-589

Chourey PS, Jain M, Li QB, Carlson SJ (2006) Genetic control of cell wall invertases in developing endosperm of maize. Planta 223:159-167

Chourey PS, Nelson OE (1996) The enzymatic deficiency conditioned by the *shrunken-1* mutations in maize. Biochem Genet 14:1041-1055

Chourey PS, Taliercio EW, Carlson SJ, Ruan YL (1998) Genetic evidence that two isozymes of sucrose synthase present un developing maize endosperm are critical, one for cell wall integrity and the other for starch biosynthesis. Mol Gen Genet 259:88-96

Ciereszko I, Kleczkowski LA (2002) Glucose and mannose regulate the expression of a major sucrose synthase gene in *Arabidopsis* via hexokinase-dependent mechanisms. Plant Phy Biochem 40:907-911

Clark KL, Larsen PB, Wang X, Chang C (1998) Association of the *Arabidopsis* CTR1 Raf-like kinase with the ETR1 and ERS ethylene receptors. Proc Natl Acad Sci USA 95:5401-5406

Creech RG (1965) Genetic control of carbohydrate synthesis in maize endosperm. Genetics 52:1175-1186

Correns, C (1901) Bastarde zwischen maisrassen, mit besonder Berucksichtung der Xenien. Bibl Bot 53, 1-161

Dai N, Schaffer AA, Petreikov M, Granot D (1995) *Arabidopsis thaliana* hexokinase cDNA isolated by complementation of yeast cells. Plant Physiol 108:879-880

Denyer K, Dunlap F, Thorbjornsen T, Keeling P, Smith AM (1996) The major form of ADP-glucose pyrophosphorylase in maize endosperm is extra-plastidial. Plant Physiol 112:7779-785

Diboll AG (1968) Fine structure development of the megagametophyte of Zea mays following fertilization. Amer J Bot 55:787-806

Dickinson DB, Preiss J (1969) ADP glucose pyrophosphorylase from maize endosperm. Arch Biochem Biophys 130:119-128

Dinges JR, Colleoni C, Myers AM, James MG (2001) Molecular structure of three mutations at the maize *sugary1* locus and their allele-specific phenotypic effects. Plant Physiol 152:1406-1418

Evensen KB, Boyer CD (1986) Carbohydrate composition and sensory quality of fresh and stored sweet corn. J Amer Soc Hort Sci 111:734-738

Foyer CH (1988) Feedback inhibition of photosynthesis through source-sink regulation in leaves. Plant Physiol Biochem 26:483-492

Gallie DR, Young TE (2004) The ethylene biosynthetic and perception machinery is differentially expressed during endosperm and embryo development in maize. Mol Gen Genet 271:267-281

Gallie DR, Geisler-Lee J, Chen J, Jolley Blair (2009) Tissue-specific expression of the ethylene biosynthetic machinery regulates root growth in maize. Plant Mol Biol 69:195-211

Gou H, Ecker JR (2003) Plant responses to ethylene gas are mediated by $SCF^{EBF1/EBF2}$-dependent proteolysis of EIN3 transcription factor. Cell 115:667-677

Grime JP, Mowforth MA (1982) Variation in genome size- an ecological interpretation. Nature 299:151-153

Hennen-Beirwagen TA, Liu F, Marsh RS, Kim S, Gan Q, Tetlow IJ, Emes MJ, James MG, Myers AM (2008) Starch biosynthetic enzymes from developing maize endosperm associate in multisubunit complexes. Plant Physiol 146:1892-1908

Hua J, Meyerowitz EM (1998) Ethylene responses are negatively regulated by a receptor gene family in *Arabidopsis thaliana*. Cell 94:261-271

James MG, Robertson DS, Myers AM (1995) Characterization of the maize gene *sugary1*, a determinant of starch composition in kernels. Plant Cell 7:417-429

Jang JC, Leon P, Zhou L, Sheen J (1997) Hexokinase as a sugar sensor in higher plants. Plant Cell 9:5-19

Jang JC, Sheen J (1994) Sugar sensing in higher plants. Plant Cell 6:1665-1679

Johnson PR, Ecker JR (1998) The ethylene gas signal transduction pathway: a molecular perspective. Annu Rev Genet 32:227-254

Kevany BM, Tieman DM, Taylor MG, Dal Sin V, Klee HJ (2007) Ethylene receptor degradation controls the timing of ripening in tomato fruit. Plant J 51:458-467

Kieber JJ, Rothenberg M, Roman G, Feldmann KA, Ecker JR (1993) CTR1, a negative regulator of the ethylene response pathway in Arabidopsis, encodes a member of the Raf family of protein kinases. Cell 72:427–41

Kiesselbach TA (1949) The structure and reproduction of corn. Univ. of Nebraska Press: Lincoln, NE

Koch KE, Nolte KD, Duke ER, McCarty DR, Avigne WT (1992) Sugar levels modulate differential expression of maize sucrose synthase genes. Plant Cell 4:59-69

Kowles RV, Phillips RL (1985) DNA amplification patterns in maize endosperm nuclei during kernel development. Proc Natl Acad Sci USA 82:7010–7014

Kowles RV, Phillips RL (1988) Endosperm development in maize. Int Rev Cytol 112:97-136

Kyle DJ, Styles ED (1977) Development of aleurone and sub-aleurone layers in maize. Planta 137:185-193

LeClere S, Schmelz EA, Chourey PS (2008) Cell wall invertase-deficient *miniature1* kernels have altered phytohormone levels. Phytochem 69:692-699

Li QB, LcClere S, Chourey P (2008) Plieotropic effects of a single-gene mutation in sucrose utilization pathway extend beyond its tissue- and metabolic-specificity in developing seed of maize. Fl Genet Conf Abstract/Poster 55

Liu Y, Zhang S (2004) Phosphorylation of 1-aminocyclopropane-1-carboxylic acid synthase by MPK6, a stress-responsive mitogen-activated protein kinase, induces ethylene biosynthesis is *Arabidopsis*. Plant Cell 16:3386-3399

Lowe J, Nelson OE Jr (1946) Miniature seed- a study in the development of a defective caryopsis in maize. Genetics 31:525-533

Lur HS, Setter TL (1993) Role of auxin in maize endosperm development. Plant Physiol 130:273-280

Maniaitis T, Fritsch EF, Sambrook J (1982) Molecular cloning: a laboratory manual. Cold Spring Harbor Laboratory, Cold Spring Harbor, New York.

Miller ME, Chourey PS (1992) The maize invertase-deficient *miniature-1* seed mutation is associated with aberrant pedicel and endosperm development. Plant Cell 4:297-305

Moore B, Zhou L, Rolland F, Hall Q, Cheng WH, Liu YX, Hwang I, Jones T, Sheen J (2003) Role of the *Arabidopsis* glucose sensor HXK1 in nutrient, light, and hormonal signaling. Science 300:332-336

Myers AM, Morell MK, James MG, Ball SG (2000) Recent progress toward understanding biosynthesis of the amylopectin crystal. Plant Physiol 122:989-997

Nelson O, Pan D (1995) Starch synthesis in maize endosperm. Annu Rev Plant Physiol Plant Mol Bio 46:475-496

Ohto M, Onai K, Furukawa Y, Aoki E, Araki T, Nakamura K (2001) Effects of sugar on vegetative development and floral transition in *Arabidopsis*. Plant Physiol 127:252-261

Pego JV, Weisbeek PJ, Smeekens SCM (1999) Mannose inhibits *Arabidopsis* germination via a hexokinase-mediated step. Plant Physiol 119:1017-1023

Preiss J, Danner S, Summers PS, Morell M, Barton CR, Yang L, Nieder M (1990) Molecular characterization of the *Brittle-2* gene effect on maize endosperm ADPglucose pyrophosphorylase subunits. Plant Physiol 92:881-885

Rahman A, Wong Ks, Jane Jl, Myers AM, Jane MG (1998) Characterization of SU1 isoamylase, a determinant of storage starch structure in maize. Plant Physiol 117:425-435

Saltman P (1953) Hexokinase in higher plants. J Biol Chem 200(1):145-154

Sebastia CH, Hardin SC, Clouse SD, Kieber JJ, Huber SC (2004) Identification of a new motif for CDPK phosphorylation in vitro that suggests ACC synthase may be a CDPK substrate. Arch Biochem Biophys 428:81-91

Shannon JC, Creech RG, Loerch JD (1970) Starch synthesis studies in *Zea mays*. Plant Physiol 45:163-168

Shannon JC, Pien FM, Cao H, Liu KC (1998) Brittle-1, an adenylate translocator, facilitates transfer of extraplastidial synthesized ADP-glucose into amyloplasts of maize endosperms. Plant Physiol 117:1235-1252

Sheen J. 1990 Metabolic repression of transcription in higher plants. Plant Cell 2:1027-1038

Shewry PR, Halford NG. (2002) Cereal seed storage proteins: structures, properties and role in grain utilization. Journal Exp Bot 53:947-958

Shure M, Wessler S, Fedoroff N (1983) Molecular identification of the *Waxy* locus in maize. Cell 35:225-233

Slein MW, Cori GT, Cori CF (1950) A comparative study of hexokinase from yeast and animal tissues. J Biol Chem 186:763-780

Tatsuki M, Mori H (2001) Phosphorylation of tomato 1-aminocyclopropane-1-carboxylic acid synthase, LeACS2, at the C-terminal region. J Biol Chem 276:28051-28057

Tsai CY, Salamini F, Nelson OE (1970) Enzymes of carbohydrate metabolism in the developing endosperm of maize. Plant Physiol 46:299–306

Vilhar B, Kladnik A, Blejec A, Chourey PS, Dermastia M (2002) Cytometrical evidence that the loss of seed weight in the *miniature1* seed mutant of maize is associated with reduced mitotic activity in the developing endosperm. Plant Physiol 129:23-30

Wu C, Colleoni C, Myers AM, James MG (2002) Enzymatic properties and regulation of ZPU1, the maize pullulanase-type starch Debranching enzyme. Arch Biochem Biophys 406:21-32

Xiao W, Sheen J, Jang JC (2000) The role of hexokinase in plant sugar signal transduction and growth and development. Plant Mol Bio 44:451-461

Yang S, Hoffman N (1984) Ethylene biosynthesis and its regulation in higher plants. Annu Rev Plant Physiol 35:155–89

Yanigisawa S, Yoo SD, Sheen J (2003) Differential regulation of EIN3 stability by glucose and ethylene signaling in plants. Nature 425:521-525

Yoo SD, Cho YH, Tena G, Xiong Y, Sheen J (2008) Dual control of nuclear EIN3 by bifurcate MAPK cascades in C_2H_4 signalling. Nature 451:789-796

Young TE, Gallie DR (2000a) Programmed cell death during endosperm development. Plant Mol Bio 44:283-301

Young TE, Gallie DR (2000b) Regulation of programmed cell death in maize endosperm by abscisic acid. Plant Mol Bio 42:397-414

Young TE, Gallie DR (2004) ACC synthase expression regulates leaf performance and drought tolerance in maize. Plant J 40:813-825

Young TE, Gallie DR, DeMason DA (1997) Ethylene-mediated programmed cell death during maize endosperm development of wild-type and *shrunken2* genotypes. Plant Physiol 115:737-751

Zhou L, Jang JC, Jones TL, Sheen J (1998) Glucose and ethylene signal transduction crosstalk revealed by an *Arabidopsis* glucose-insensitive mutant. Proc Natl Acad Sci 95:10294-10299

BIOGRAPHICAL SKETCH

Andrew Joseph Funk was born to Joseph William and Donna Carol Funk during the year 1983 in the town of Decatur, IL. In 1990 he moved with his parents and sister to Tallahassee, FL. During high school he developed a love for biology under the teaching of Janice Ouimet. This led to his receipt of a bachelor's degree in microbiology and cell science from the University of Florida in 2006, where he worked as a research assistant in the laboratory of Dr. Prem Chourey. At Dr. Chourey's invitation, Andrew applied to the plant pathology program at the University of Florida, and worked for the United States Department of Agriculture while fulfilling requirements for the degree of Master of Science.